DATA REPORT

SkyTEM Survey: Limoges, France

Client: BRGM

Date: November 2022

AIRBORNE SURVEYS WORLDWIDE

SKYTEM SURVEYS APS
DYSSEN 2
8200 AARHUS N, DENMARK

TEL: +45 8620 2050
VAT: 27704379

SKYTEM.COM
INFO@SKYTEM.COM

Structure of the Digital Data Delivery catalogue

Folder	Sub folders		File format	Content
01_Data	01_GDB		.gdb (Geosoft database)	AUX_MAG_EM data
	02_Workbench	01_Data	.xyz, .sps(Ascii file) .gex (settings file) .alc (import template) .lin (mask file)	Files for import of xyz data to Workbench
		02_gex		
		03_Alc		
		04_Lin		
	03_PFC_parameters		.dat (ascii file)	PFC parameters
	04_Rawdata		.mat	Raw EM data
02_Inversion	01_GDB_Models		.gdb (Geosoft database)	Modelled layer resistivity
	02_Layer_resistivity_Grids		.grd (Geosoft grid)	Modelled layer resistivity
	03_Layer_resistivity_Maps		.map (Geosoft map) .pdf	Modelled layer resistivity
	04_Layer_resistivity_Profiles		.png	Profile sections of modelled layer resistivity & model analysis
03_Maps	01_DEM		.map (Geosoft maps), .pdf	DEM
	02_FlightPath		.map (Geosoft maps), .pdf	Flight path
	03_PlannedFlightLines		.map (Geosoft maps), .pdf	Planned flightlines
	04_MAG		.map (Geosoft maps), .pdf	RMF & TMI
	05_EM_HeightCor		.map (Geosoft maps), .pdf	Height Corrected EM gates
	06_EM_B-field		.map (Geosoft maps), .pdf	B-field channels
	07_PLNI_Tau		.map (Geosoft maps), .pdf	PLNI & Tau
04_Grids	01_DEM		.grd (Geosoft grid)	DEM
	02_MAG		.grd (Geosoft grid)	RMF & TMI
	03_EM_HeightCor		.grd (Geosoft grid)	Height Corrected EM gates
	04_EM_B-field		.grd (Geosoft grid)	B-field channels
	05_PLNI_Tau		.grd (Geosoft grid)	PLNI & Tau
05_Report			.pdf	Data report

Contents

Executive Summary

This report covers data acquisition, technical specifications, data processing and presentation of the SkyTEM306HPM survey flown in the period from June 27th to August 11th 2022 near Limoges, France.

The survey is a part of a survey campaign inlcuding two other areas, Clermont Ferrand and Castres, that are described in separate reports.

The survey is comprised of 1 block containing a total of 7130.8 km planned flight lines.

The SkyTEM306HPM system collects time domain electromagnetic and magnetic data along with supporting navigation measurements.

All materials are delivered digitally. The final product includes:

- Data report
- Processed data in a Geosoft database format
- Inversion results; modelled layer resistivity in Geosoft database format
- Grids and maps in Geosoft format
- Presentations of data and inversion results in png or pdf format

An overview of the digital data delivery can be seen on the first page in the report.

This report does not include any geological interpretations of the geophysical dataset.

Survey outline

The survey area is located to the North side of Limoges, France. The planned survey lines are presented as blue lines on Figure 1 and have a line spacing of 400 m in an E-W direction. The tie lines have a line spacing of 4000 m in a N-S direction. Flight line details are listed in Table 1 and Table 2. A test line were flown in the survey area to determine the optimal data acquisition script. The survey was flown from June 27th to August 11th 2022.

Actual flown lines (red lines) versus planned lines (blue lines) are presented in Figure 2. Discrepancies between planned and flown lines can occur where cultural features such as roads, buildings or powerlines necessitated a diversion from the planned lines.

The coordinate system UTM Zone UTM31N (WGS84) is used throughout this report, and in the data delivery.

Acquisition system	Area	Spacing m	Direction (in- /tie lines)	Number of Lines	Total km
SkyTEM306HPM	Limoges	400 / 4000	E - W / N – S	466 / 40	6358.5 / 663.6
	Rochehouart	-	-	6	108.7
	In Total				7130.8 km

Table 1 Survey details

Acquisition system	Area	Line numbering (in- / tie lines)
SkyTEM306HPM	Limoges	200000 – 206520 / 290000 - 297200
	Rochehouart	270000 - 270500
	Reference line	921001 – 921055, 922001 – 922002, 923001 - 923009
	Bias line	930001 – 930011, 940012 - 940066

Table 2 Line numbering

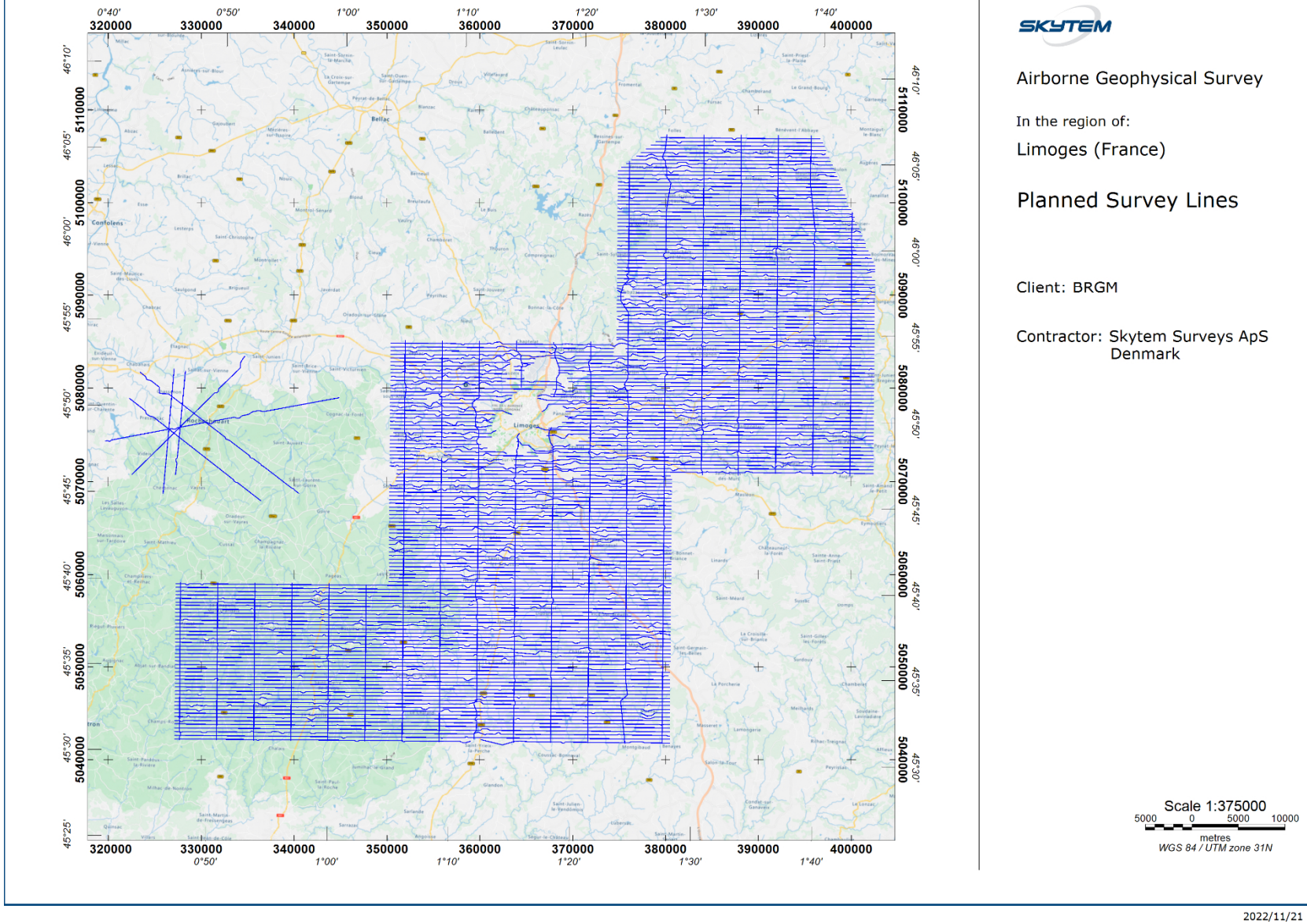

Figure 1. Planned survey lines in blue for the SkyTEM306HPM system

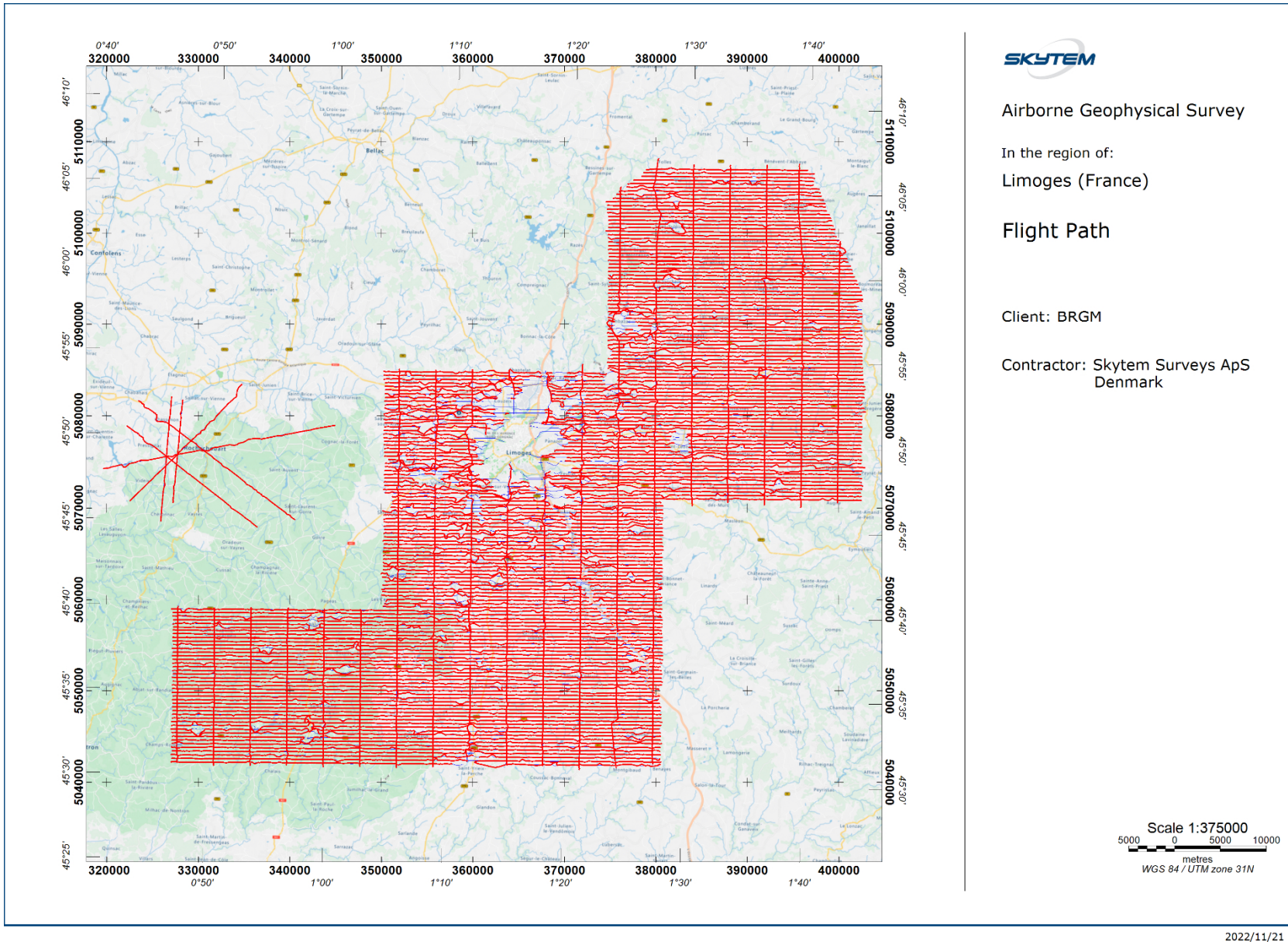

Figure 2 Planned survey lines in blue superimposed by actual flown lines in red by SkyTEM306HPM system.

Introduction

The SkyTEM electromagnetic and magnetic survey described in this report is flown with the SkyTEM306HPM system.
The survey was requested by BRGM and performed by SkyTEM Surveys ApS. Basic survey information and key personnel are listed in Table 3.

This report covers data acquisition, instrument descriptions, data processing and presentations. The data delivery includes processed electromagnetic data and presentations, spatially constrained inversion results (SCI), model presentations as well as processed magnetic data and presentations. The digital data delivery folder is described in the front inside cover of this report.

This report does not include any geological interpretations of the geophysical dataset.

BRGM (Client)	
Client Contact person	Mr Guillaume Martelet Email: g.martelet@brgm.fr
SkyTEM Surveys ApS (Contractor)	
Contact person	Mr Flemming Effersø Email: fe@skytem.com
Project Manager	Mr Per Gisselø Email: pgg@skytem.com
Field Crew	Mr Gorm Thøgersen Mr Christian Sodemann Mr Emil Nielsen
KMN Koopmann Helicopter gmbh (Helicopter operator)	
Helicopter type	Eurocopter Astar 350 B3
Pilots	Mr Franz Schmidt Mr Christian Pfeifhofer Mr Walter Koopmann
Data acquisition period	June 27th to August 11th 2022
Data processing, presentations, and report	Mr Per Gisselø

Table 3 Key personnel and survey information.

Flight Parameters

The nominal terrain clearance of the transmitter is 35 - 45 m, with an increase in flight height over forests, power lines, or any other obstacles or hazards. The safe flying height during the survey is always based on the pilot's assessment of risk and deviations from nominal values are at the discretion of the pilot.

The nominal production airspeed was 60 - 80 kph for a flat topography with no wind. This may vary in areas of rugged terrain and/or windy conditions.

Average values and standard deviations of survey flight parameters are found in Table 4.

SkyTEM306HPM:

Control parameter		Average Value	Standard Deviation
Ground speed*)		73.7 kph	9.3 kph
Processed height		59.3 m	14.7 m
Tilt angle	X	0.7 degrees	2.8 degrees
	Y	-0.1 degrees	1.5 degrees
High Moment Current		226.3 Amp	5.6 Amp
Low Moment Current		7.88 Amp	0.03 Amp

Table 4 Flight parameters

**) Actual speed varies as a function of day and flight direction due to different wind directions and magnitude.*

Flight Reports

For each flight, a report with key information regarding the data acquisition is made in the field. Listed in the reports are details on the weather, special data parameters and other events which may influence the data. Weather report and flight report can be seen in Table 5 and Table 6, respectively.

Flight	Temperature (C)	Wind (knots)	Visibility
20220627.01	23	2-4N	Good
20220627.02	25	low	Good
20220628.01	15	low	Good
20220628.02	25	low	Good
20220629.01	18	low	Good
20220629.02	25	low	Good
20220701.01	15	low	Good
20220701.02	18	low	Good
20220702.01	18	low	Good
20220704.01	21	3 NW	Good
20220704.02	22	3 NW	Good
20220705.01	20	2 N	Good
20220705.02	25	3 NW	Good
20220706.01	17	2 NE	Good
20220706.02	23	3 NE	Good
20220707.01	15	2 N	Good
20220707.02	22	4 N	Good
20220707.03	25	4 N	Good
20220708.01	15	4 NE	Good
20220708.02	22	3 NE	Good
20220708.03	22	3 NE	Good
20220709.01	18	3 NE	Good
20220711.01	20	3 NE	Good
20220711.02	27	4 NE	Good
20220712.01	19	3 E	Good
20220712.02	28	4 NE	Good
20220713.01	19	2 NE	Good
20220714.01	23	1 S	Good
20220714.02	29	3 SE	Good
20220715.01	19	1 SE	Good
20220715.02	28	3 S	Good
20220716.01	26	2 E	Good
20220716.02	24	3 NE	Good
20220718.01	32	2 E	Good
20220719.01	32	4 SE	Good

20220719.02	31	3 SE	Good
20220720.01	18	2 NE	Okay
20220720.02	21	0 N	Good
20220720.03	23	4 SE	Good
20220721.01	18	2 NE	Okay
20220721.02	25	2 NE	Good
20220722.01	19	3 NE	Good
20220726.01	19	2 NW	Good
20220726.02	19	2 NE	Good
20220727.01	17	2 NE	Good
20220727.02	26	2 NE	Good
20220727.03	25	2 NE	Good
20220728.01	18	2 SW	Good
20220728.02	26	2 SW	Good
20220729.01	18	1 W	Okay
20220709.02	24	3 SE	Good
20220730.01	18	1 NW	Good
20220730.02	26	1 W	Good
20220801.01	20	1 NE	Good
20220801.02	30	2 NW	Good
20220802.01	20	2 NE	Good
20220802.02	27	2 NE	Good
20220803.01	23	1 E	Good
20220804.01	30		Good
20220804.02	37		Good
20220805.01	22	Low	Good
20220805.02	30		Good
20220806.01	22	4-6 NE	Good
20220806.02	25	6-8 NE	Good
20220808.01	25	4-6 NE	Good
20220808.02	30	6-8 NE	Good
20220809.01	20	4-6 NE	Good
20220809.02	25	5-7 NE	Good
20220810.01	28	4-6 NE	Good
20220810.02	32	5-7 NE	Good
20220811.01	20	Low	Good
20220811.02	30	Low	Good

Table 5 Weather report

Flight	Comments
20220627.01	Production
20220627.02	Production
20220628.01	Production
20220628.02	Production
20220629.01	Production
20220629.02	Production
20220701.01	Production
20220701.02	Production
20220702.01	Production
20220704.01	Production. Cut short due to rain.
20220704.02	Production
20220705.01	Production. Generator failed
20220705.02	Production
20220706.01	Production
20220706.02	Production
20220707.01	Production
20220707.02	Production
20220707.03	Recon flight
20220708.01	Production
20220708.02	Production
20220708.03	Recon flight
20220709.01	Reflights - Limoges block
20220711.01	Production (partially failed)
20220711.02	Production (failed, but one line recovered)
20220712.01	Production
20220712.02	Production
20220713.01	Production
20220714.01	Production
20220714.02	Production
20220715.01	Production
20220715.02	Production
20220716.01	Production. Generator stopped mid-air.
20220716.02	Production
20220718.01	Production
20220719.01	Production. Aborted due to fuel-filter warning in helicopter. No Bias test.
20220719.02	Production
20220720.01	Production
20220720.02	Flight aborted, due to no cooling.
20220720.03	Production
20220721.01	Production

20220721.02	Production. Moved to Nexon.
20220722.01	Production
20220726.01	Production
20220726.02	Aborted. Changed generator.
20220727.01	Production
20220727.02	Production
20220727.03	Production
20220728.01	Production
20220728.02	Production
20220729.01	Production. System stopped mid-air.
20220709.02	Production
20220730.01	Production
20220730.02	Production
20220801.01	Production
20220801.02	Production
20220802.01	Production
20220802.02	Production. Generator stopped mid-air
20220803.01	Production. Generator stopped mid-air
20220804.01	Production
20220804.02	Production
20220805.01	Production
20220805.02	Production
20220806.01	Production
20220806.02	Production. Short flight system stopped mid-air.
20220808.01	Production
20220808.02	Production
20220809.01	Production
20220809.02	Production
20220810.01	Production
20220810.02	Production
20220811.01	Production
20220811.02	Production

Table 6 Flight report.

Instruments

This section provides an overview of airborne as well as ground base instruments, thorough technical descriptions are provided in Appendix 1.

Airborne unit

The airborne instrumentation comprising a SkyTEM306HPM system includes a time domain electromagnetic system, a magnetic data acquisition system and an auxiliary data acquisition system containing two inclinometers, two altimeters and three DGPS'. All instruments are mounted on the frame suspended ~40 m below the helicopter, the generator used to power the transmitter is suspended between the frame and the helicopter, ~30 m below the helicopter. A picture of the airborne SkyTEM system is seen on Figure 3, and a sketch of the instrumentation is seen on Figure 4.

Figure 3 SkyTEM System airborne

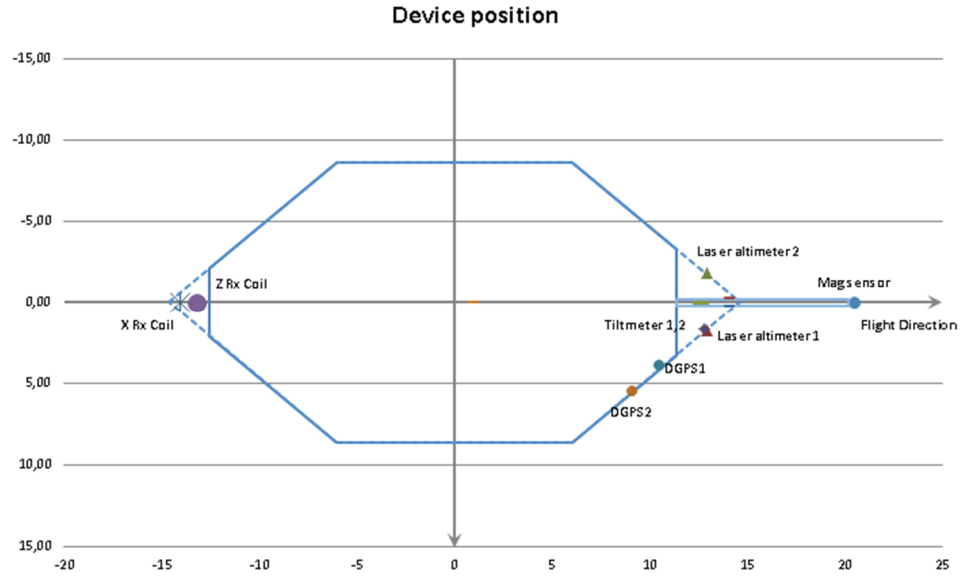

Figure 4 Sketch showing the frame and the position of the basic instruments. The blue line defines the transmitter loop. The horizontal plane is defined by (x,y).

Ground base stations

The magnetic base stations were positioned in the vicinity of the landing site.

DGPS base station

DGPS base stations were placed at a location of maximum possible view to satellites and away from metallic objects that could influence the GPS antenna.

GPS processing involves a Precise Point Positioning (PPP) setup using the L1 and L2 band of the GPS rover. The PPP process eliminates the need of base station data and the improved precision obtained during the post-processing is based on correction and precision files which are downloaded during the processing steps.

DGPS base station data is only acquired for backup and was not used in the processing on this survey.

Limoges – 20220627 to 20220721

ID #	Latitude	Longitude	Height
BGPS 12078	45.743765°	1.384673°	311.98 m
BGPS 12080	45.743810°	1.384715°	312.30 m

Nexon – 20220722 to 20228011

ID #	Latitude	Longitude	Height
BGPS 12078	45.670603°	1.183668°	414.43 m
BGPS 12080	46.670588°	1.183873°	415.29 m

Magnetometer base station

The base station magnetometer was placed in a location of low magnetic gradient, away from electrical transmission lines and moving metallic objects, such as motor vehicles and aircrafts.

Limoges – 20220627 to 20220721

ID #	Status	Latitude	Longitude	Height
Bmag 08792	Primary	45.744835°	1.386453°	654 m
Bmag 05021	Backup	45.744835°	1.386880°	309 m

Nexon – 20220722 to 20228011

ID #	Status	Latitude	Longitude	Height
Bmag 08792	Primary	45.671333°	1.185690°	403 m
Bmag 05021	Backup	45.671665°	1.185830°	404 m

Data Acquisition

The SkyTEM306HPM system setup is a dual moment configuration containing a High Moment (HM) with a peak moment of ~ 500,000 NIA and a Low Moment (LM) with a peak moment of ~3,000 NIA.

Data from two DGPS receivers are recorded by the EM data acquisition system while a third DGPS is recorded by the magnetic data acquisition system. The DGPS systems are used for time stamping, positioning, and correlation of the EM and magnetic datasets. All recorded data are marked with a time stamp used to link the different data types. One GPS receiver on the frame is activated for Precise Point Positioning (PPP) processing, which allows for a precise processing of the GPS position without the need of the base station GPS.

The time stamp is in UTC/GMT and the formats are either,

- Date and Time defined as; yyyy/mm/dd hh:mm:ss.sss
  or
- Datetime values defined as the number of decimal days since 1900-01-01; ddddd.dddddd

Gate times

The gate times for the SkyTEM306HPM system are found in the following tables.

Gate times for all the measured Low moment gates on the SkyTEM306HPM system are presented in Table 7. Gate 1 – 20 of the LM gates were corrected for the primary field allowing the use of earlier gates than otherwise possible and are represented by boxcar gates. Gate 21 to 51 are provided as tapered gate values, where the gate tapering results in improved suppression of high frequency noise in the data. The times refer to beginning of ramp down.

Gate times for the merged Low moment gates on the SkyTEM306HPM system are presented in Table 8. Gate 1 – 16 of the LM gates were corrected for the primary field allowing the use of earlier gates than otherwise possible and are represented by boxcar gates. The original gates 17 to 51 has been merged into new wider gates reducing the gate span to cover gate numbers 17 to 34. These gates are provided as merged tapered gate values, where the merging and gate tapering results in improved suppression of high frequency noise in the data. The times refer to beginning of ramp down.

The High moment data on SkyTEM306HPM are provided as tapered gate values, where the gate tapering results in improved suppression of high frequency noise in the data. The equivalent gate times of the tapered gates are presented in Table 9 for the SkyTEM306HPM. The times refer to the end of ramp.

The tapered gates constitute smooth weighing functions which are applied to the recorded dB/dt signals with overlap between neighbouring gates. The weighing functions used are B-splines of order 3, which means that they are piecewise polynomial functions of order 2. The B-spline has been chosen specifically for the purpose of weighing function due to its property of:

- being maximally smooth while being compact (resulting in superior low pass filtering qualities),
- in combination the set of gates ensure equal weighing of the entire sounding curve,
- being uniquely defined simply by the chosen set of gate transition times (also called knot points),
- associated expressions exist for its function moments and frequency transform

The standard LM tapered gates are generated with gate transition times/knot points located at the gate transitions of the box gates.
The wider/merged LM tapered gates are generated with gate transition times/knot points located at every second gate transition of the box gates.
This means that every standard LM tapered gate contains signal contributions from three neighbouring box gate intervals, while every wide/merged LM tapered gate contains signal contributions from six neighbouring box gate intervals.

The B field channels represent the actual B field level at the given channel time. Channel times for system SkyTEM306HPM can be found in Table 10.

The earliest gates, defined in Table 7 to Table 10, are not used as these are in the transition zone and affected by the primary field of the transmitter.

The calibration parameters for

SkyTEM306HPM
Low Moment
Shift factor: 1.0 (on the raw dB/dt data)
Time shift: 0.6e-6 s

High Moment
Shift factor: 1.0 (on the raw dB/dt data)
Time shift: 0.0e-6 s

Gate #	Gate Center (s)	Gate Open (s)	Gate Close (s)	Comment
1	3.000E-07	0.000E+00	6.000E-07	Not used
2	1.000E-06	6.000E-07	1.400E-06	Not used
3	1.700E-06	1.400E-06	2.000E-06	Not used
4	2.400E-06	2.000E-06	2.800E-06	LM
5	3.200E-06	2.800E-06	3.600E-06	LM
6	4.000E-06	3.600E-06	4.400E-06	LM
7	4.800E-06	4.400E-06	5.200E-06	LM
8	5.700E-06	5.200E-06	6.200E-06	LM
9	6.600E-06	6.200E-06	7.000E-06	LM
10	7.600E-06	7.000E-06	8.200E-06	LM
11	8.700E-06	8.200E-06	9.200E-06	LM
12	9.800E-06	9.200E-06	1.040E-05	LM
13	1.110E-05	1.040E-05	1.180E-05	LM
14	1.250E-05	1.180E-05	1.320E-05	LM
15	1.400E-05	1.320E-05	1.480E-05	LM
16	1.570E-05	1.480E-05	1.660E-05	LM
17	1.750E-05	1.660E-05	1.840E-05	LM
18	1.940E-05	1.840E-05	2.040E-05	LM
19	2.160E-05	2.040E-05	2.280E-05	LM
20	2.410E-05	2.283E-05	2.537E-05	LM
21	2.675E-05	2.538E-05	2.812E-05	LM
22	2.965E-05	2.812E-05	3.118E-05	LM
23	3.290E-05	3.120E-05	3.460E-05	LM
24	3.645E-05	3.458E-05	3.832E-05	LM
25	4.040E-05	3.833E-05	4.247E-05	LM
26	4.475E-05	4.248E-05	4.702E-05	LM
27	4.950E-05	4.700E-05	5.200E-05	LM
28	5.480E-05	5.203E-05	5.757E-05	LM
29	6.060E-05	5.757E-05	6.363E-05	LM
30	6.700E-05	6.363E-05	7.037E-05	LM
31	7.410E-05	7.040E-05	7.780E-05	LM
32	8.190E-05	7.780E-05	8.600E-05	LM
33	9.055E-05	8.602E-05	9.508E-05	LM
34	1.001E-04	9.510E-05	1.051E-04	LM
35	1.107E-04	1.051E-04	1.162E-04	LM
36	1.224E-04	1.162E-04	1.285E-04	LM
37	1.353E-04	1.285E-04	1.420E-04	LM
38	1.496E-04	1.421E-04	1.571E-04	LM
39	1.654E-04	1.571E-04	1.736E-04	LM
40	1.828E-04	1.736E-04	1.919E-04	LM
41	2.020E-04	1.919E-04	2.121E-04	LM
42	2.233E-04	2.121E-04	2.344E-04	LM
43	2.468E-04	2.344E-04	2.591E-04	LM
44	2.728E-04	2.591E-04	2.864E-04	LM
45	3.015E-04	2.864E-04	3.165E-04	LM
46	3.332E-04	3.166E-04	3.498E-04	LM
47	3.682E-04	3.498E-04	3.866E-04	LM
48	4.069E-04	3.866E-04	4.272E-04	LM
49	4.498E-04	4.273E-04	4.722E-04	LM
50	4.907E-04	4.702E-04	5.112E-04	LM
51	5.218E-04	5.085E-04	5.350E-04	LM

Table 7. SkyTEM306HPM. LM Gate times with respect to the beginning of ramp down.

Gate #	Gate Center (s)	Gate Open (s)	Gate Close (s)	Comment
1	3.000E-07	0.000E+00	6.000E-07	Not used
2	1.000E-06	6.000E-07	1.400E-06	Not used
3	1.700E-06	1.400E-06	2.000E-06	Not used
4	2.400E-06	2.000E-06	2.800E-06	LM
5	3.200E-06	2.800E-06	3.600E-06	LM
6	4.000E-06	3.600E-06	4.400E-06	LM
7	4.800E-06	4.400E-06	5.200E-06	LM
8	5.700E-06	5.200E-06	6.200E-06	LM
9	6.600E-06	6.200E-06	7.000E-06	LM
10	7.600E-06	7.000E-06	8.200E-06	LM
11	8.700E-06	8.200E-06	9.200E-06	LM
12	9.800E-06	9.200E-06	1.040E-05	LM
13	1.110E-05	1.040E-05	1.180E-05	LM
14	1.250E-05	1.180E-05	1.320E-05	LM
15	1.400E-05	1.320E-05	1.480E-05	LM
16	1.570E-05	1.480E-05	1.660E-05	LM
17	1.885E-05	1.685E-05	2.085E-05	LM merge
18	2.330E-05	2.090E-05	2.570E-05	LM merge
19	2.870E-05	2.573E-05	3.167E-05	LM merge
20	3.530E-05	3.170E-05	3.890E-05	LM merge
21	4.330E-05	3.893E-05	4.767E-05	LM merge
22	5.305E-05	4.775E-05	5.835E-05	LM merge
23	6.490E-05	5.843E-05	7.137E-05	LM merge
24	7.935E-05	7.145E-05	8.725E-05	LM merge
25	9.700E-05	8.737E-05	1.066E-04	LM merge
26	1.186E-04	1.068E-04	1.303E-04	LM merge
27	1.449E-04	1.305E-04	1.593E-04	LM merge
28	1.771E-04	1.595E-04	1.946E-04	LM merge
29	2.164E-04	1.949E-04	2.378E-04	LM merge
30	2.643E-04	2.381E-04	2.905E-04	LM merge
31	3.229E-04	2.909E-04	3.549E-04	LM merge
32	3.944E-04	3.553E-04	4.335E-04	LM merge
33	4.605E-04	4.269E-04	4.941E-04	LM merge
34	5.109E-04	4.902E-04	5.316E-04	LM merge

Table 8. SkyTEM306HPM. LM merged gate times with respect to the beginning of ramp down.

Gate #	Gate Center (s)	Gate Open (s)	Gate Close (s)	Comment
1	7.000E-07	1.409E-18	1.400E-06	Not used
2	2.150E-06	1.417E-06	2.883E-06	Not used
3	3.700E-06	2.900E-06	4.500E-06	Not used
4	5.400E-06	4.500E-06	6.300E-06	Not used
5	7.300E-06	6.300E-06	8.300E-06	Not used
6	9.500E-06	8.333E-06	1.067E-05	HM
7	1.210E-05	1.070E-05	1.350E-05	HM
8	1.515E-05	1.348E-05	1.682E-05	HM
9	1.885E-05	1.685E-05	2.085E-05	HM
10	2.330E-05	2.090E-05	2.570E-05	HM
11	2.870E-05	2.573E-05	3.167E-05	HM
12	3.530E-05	3.170E-05	3.890E-05	HM
13	4.330E-05	3.893E-05	4.767E-05	HM
14	5.305E-05	4.775E-05	5.835E-05	HM
15	6.490E-05	5.843E-05	7.137E-05	HM
16	7.935E-05	7.145E-05	8.725E-05	HM
17	9.700E-05	8.737E-05	1.066E-04	HM
18	1.186E-04	1.068E-04	1.303E-04	HM
19	1.449E-04	1.305E-04	1.593E-04	HM
20	1.771E-04	1.595E-04	1.946E-04	HM
21	2.164E-04	1.949E-04	2.378E-04	HM
22	2.643E-04	2.381E-04	2.905E-04	HM
23	3.229E-04	2.909E-04	3.549E-04	HM
24	3.944E-04	3.553E-04	4.335E-04	HM
25	4.818E-04	4.340E-04	5.295E-04	HM
26	5.885E-04	5.302E-04	6.467E-04	HM
27	7.188E-04	6.476E-04	7.899E-04	HM
28	8.779E-04	7.910E-04	9.648E-04	HM
29	1.072E-03	9.661E-04	1.178E-03	HM
30	1.310E-03	1.180E-03	1.439E-03	HM
31	1.600E-03	1.441E-03	1.758E-03	HM
32	1.954E-03	1.760E-03	2.147E-03	HM
33	2.387E-03	2.150E-03	2.623E-03	HM
34	2.915E-03	2.626E-03	3.204E-03	HM
35	3.560E-03	3.208E-03	3.913E-03	HM
36	4.349E-03	3.918E-03	4.779E-03	HM
37	5.311E-03	4.786E-03	5.837E-03	HM
38	6.487E-03	5.845E-03	7.130E-03	HM
39	7.924E-03	7.139E-03	8.708E-03	HM
40	9.399E-03	8.627E-03	1.017E-02	HM
41	1.056E-02	1.004E-02	1.107E-02	HM

Table 9 SkyTEM306HPM: HM gate times referenced to the end of ramp down.

Channel number #	Channel time (s)	Comment
1	1.4000E-06	Not used
2	2.8000E-06	Not used
3	4.4000E-06	Not used
4	6.2000E-06	Not used
5	8.2000E-06	Not used
6	1.0400E-05	HM B-field
7	1.3200E-05	HM B-field
8	1.6600E-05	HM B-field
9	2.0400E-05	HM B-field
10	2.5200E-05	HM B-field
11	3.1000E-05	HM B-field
12	3.8200E-05	HM B-field
13	4.6800E-05	HM B-field
14	5.7200E-05	HM B-field
15	7.0000E-05	HM B-field
16	8.5600E-05	HM B-field
17	1.0460E-04	HM B-field
18	1.2780E-04	HM B-field
19	1.5620E-04	HM B-field
20	1.9100E-04	HM B-field
21	2.3320E-04	HM B-field
22	2.8500E-04	HM B-field
23	3.4800E-04	HM B-field
24	4.2520E-04	HM B-field
25	5.1940E-04	HM B-field
26	6.3440E-04	HM B-field
27	7.7480E-04	HM B-field
28	9.4640E-04	HM B-field
29	1.1560E-03	HM B-field
30	1.4118E-03	HM B-field
31	1.7246E-03	HM B-field
32	2.1064E-03	HM B-field
33	2.5728E-03	HM B-field
34	3.1424E-03	HM B-field
35	3.8382E-03	HM B-field
36	4.6880E-03	HM B-field
37	5.7258E-03	HM B-field
38	6.9936E-03	HM B-field
39	8.5420E-03	HM B-field
40	1.0433E-02	HM B-field

Table 10 SkyTEM306HPM HM B-field channel times are referenced to end of ramp down.

Waveform

The waveforms for LM and HM are measured using a Rogowski coil on the SkyTEM306HPM system. An approximation to the measured waveform is applied in modelling of the EM data.

SkyTEM306HPM:

Figure 5 and Figure 6 show the approximated up- and down ramp of the waveform. Details are presented in Table 11 and Table 12.

Waveform tables are found in Table 13 and Table 14.

Parameter	Value
Base frequency	25 Hz
Current range	8 Amp

Table 11: Waveform parameters for LM

Parameter	Value
Base frequency	25 Hz
Current range	225 Amp

Table 12: Waveform parameters for HM

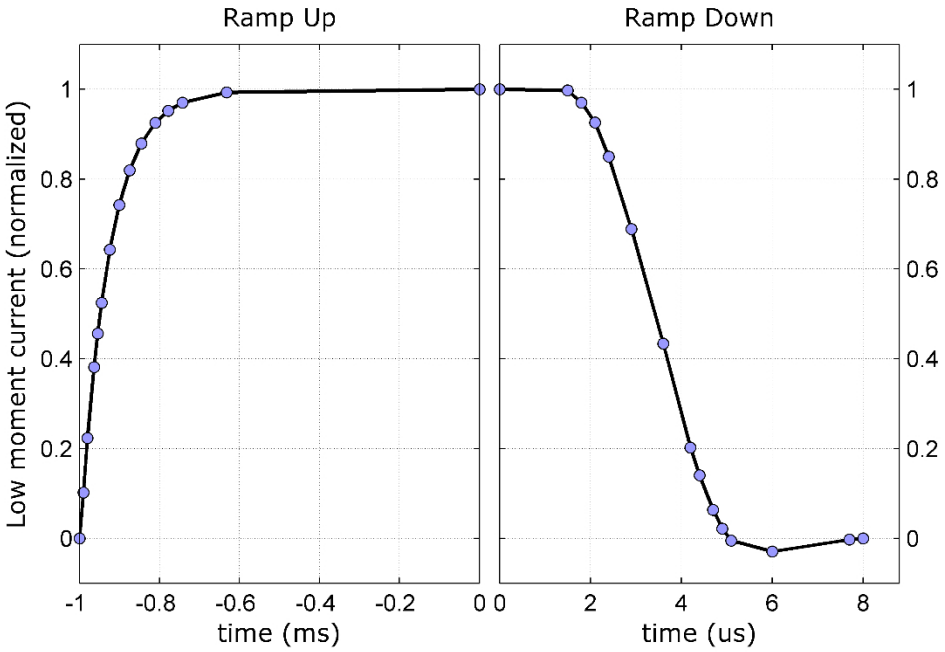

Figure 5. Ramp up and down for the LM waveform. The current is normalised.

Time [s]	Normalized current
-9.99400E-04	0.00000E+00
-9.90100E-04	1.01858E-01
-9.79800E-04	2.23472E-01
-9.63600E-04	3.81255E-01
-9.54400E-04	4.55856E-01
-9.44700E-04	5.24655E-01
-9.24100E-04	6.42971E-01
-9.00500E-04	7.42463E-01
-8.74700E-04	8.19646E-01
-8.45500E-04	8.79326E-01
-8.10600E-04	9.25233E-01
-7.77800E-04	9.52200E-01
-7.42200E-04	9.70510E-01
-6.32400E-04	9.93028E-01
0.00000E+00	1.00000E+00
1.50000E-06	9.97514E-01
1.80000E-06	9.70432E-01
2.10000E-06	9.26306E-01
2.40000E-06	8.50204E-01
2.90000E-06	6.89170E-01
3.60000E-06	4.33874E-01
4.20000E-06	2.02393E-01
4.40000E-06	1.40325E-01
4.70000E-06	6.34622E-02
4.90000E-06	2.16916E-02
5.10000E-06	-5.21350E-03
6.00000E-06	-2.93637E-02
7.70000E-06	-2.81983E-03
8.00000E-06	0.00000E+00

Table 13: Normalized current waveform for LM

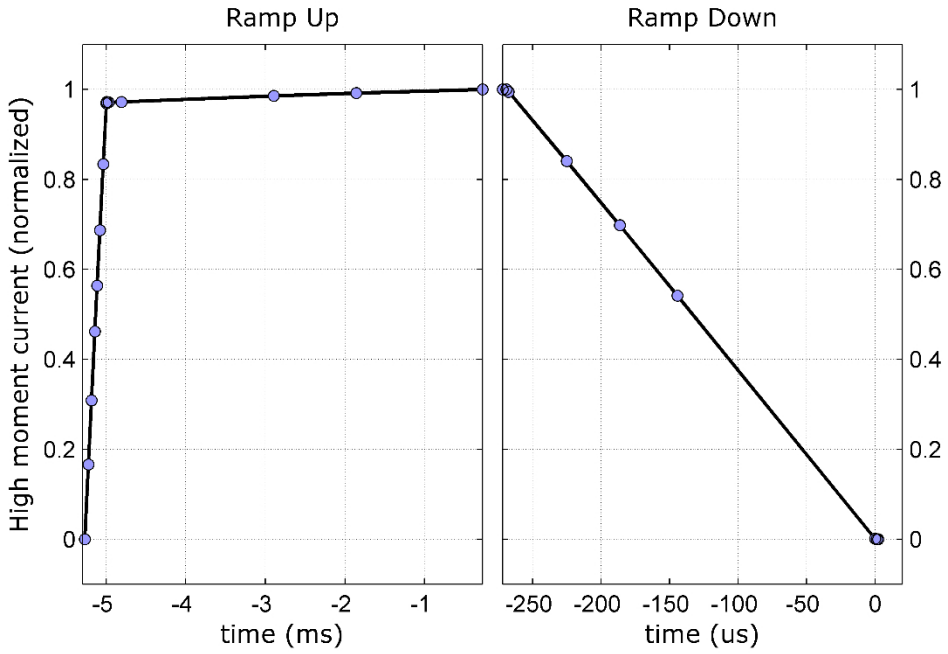

Figure 6. Ramp up and down for the HM waveform. The current is normalised.

Time [s]	Normalized current
-5.27060E-03	0.00000E+00
-5.22520E-03	1.66057E-01
-5.18640E-03	3.08500E-01
-5.14420E-03	4.61733E-01
-5.11580E-03	5.63674E-01
-5.08100E-03	6.87072E-01
-5.03880E-03	8.34127E-01
-4.99920E-03	9.69165E-01
-4.99760E-03	9.72168E-01
-4.99160E-03	9.71574E-01
-4.97100E-03	9.71472E-01
-4.81100E-03	9.72128E-01
-2.89560E-03	9.85532E-01
-1.85960E-03	9.91929E-01
-2.72000E-04	1.00000E+00
-2.69200E-04	9.99820E-01
-2.67600E-04	9.94751E-01
-2.25200E-04	8.40685E-01
-1.86400E-04	6.97941E-01
-1.44200E-04	5.41170E-01
0.00000E+00	9.13956E-04
1.40000E-06	-3.52615E-04
2.40000E-06	0.00000E+00

Table 14: Normalized current waveform for HM

High Altitude Flights

Data with SkyTEM306HP were recorded with a production script in 1000 masl on two flights during the survey campaign. The flights are 20220617.03 and 20220812.01. Data from the two flights can be seen on Figure 7 and Figure 8 respectively. From left to right the four panels show LM Z uncorrected data, LM Z PFC corrected data, HM Z data, and HM X data. Data were recorded with the transmitter TX on in an altitude free of signal from the ground. Hence, only the system itself, outcoming noise sources e.g. radio transmitters will be seen in the recorded data.
Individual sounding curves with the transmitter on are shown in grey.
The blue lines show the mean (μ) of the signal with the transmitter turned on. The stippled blue curve show the standard deviation (σ) on the EM data.

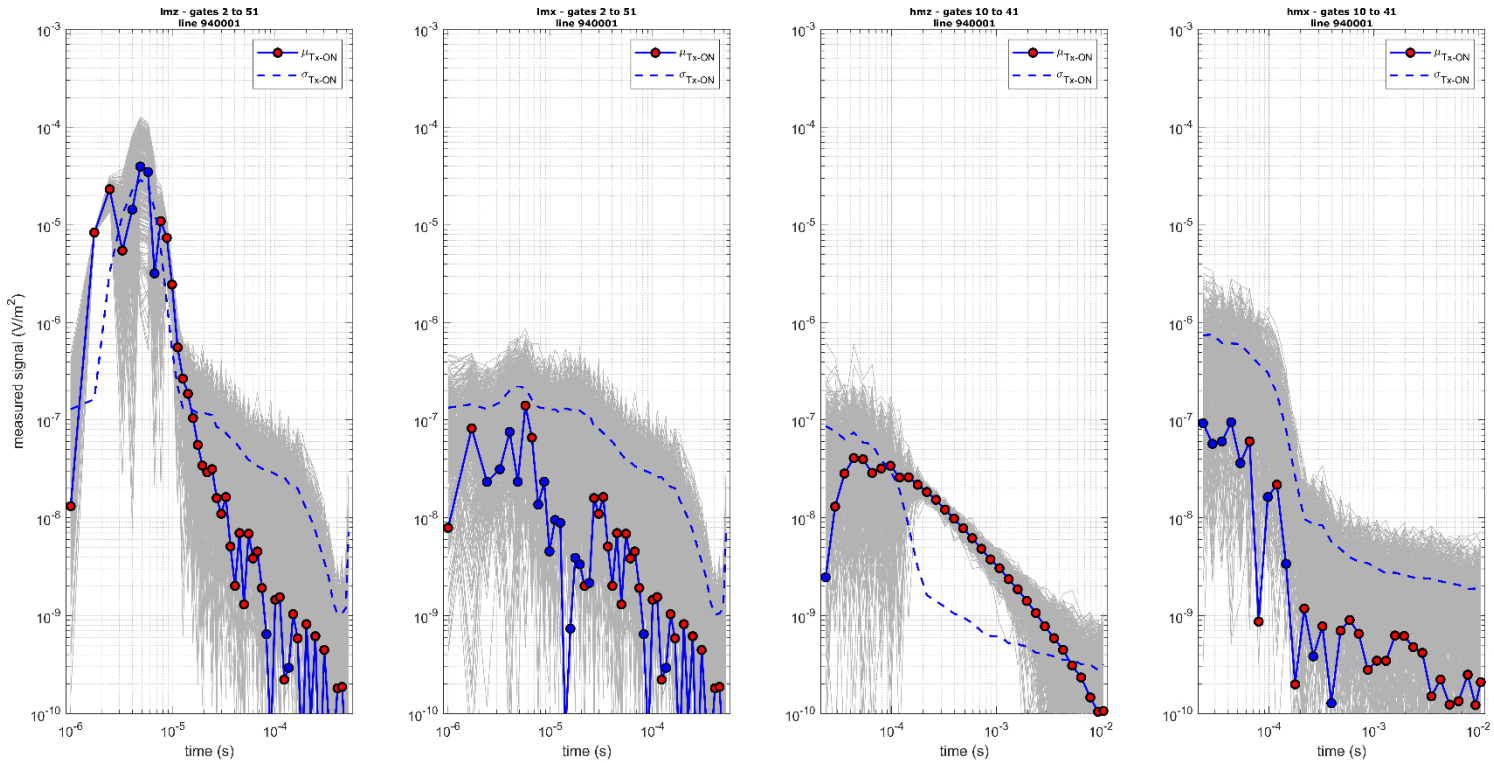

Figure 7 SkyTEM306HP high altitude data from flight 20220617.03. From left to right the four panels show LM Z uncorrected data, LM Z PFC corrected data, HM Z data, and HM X data.

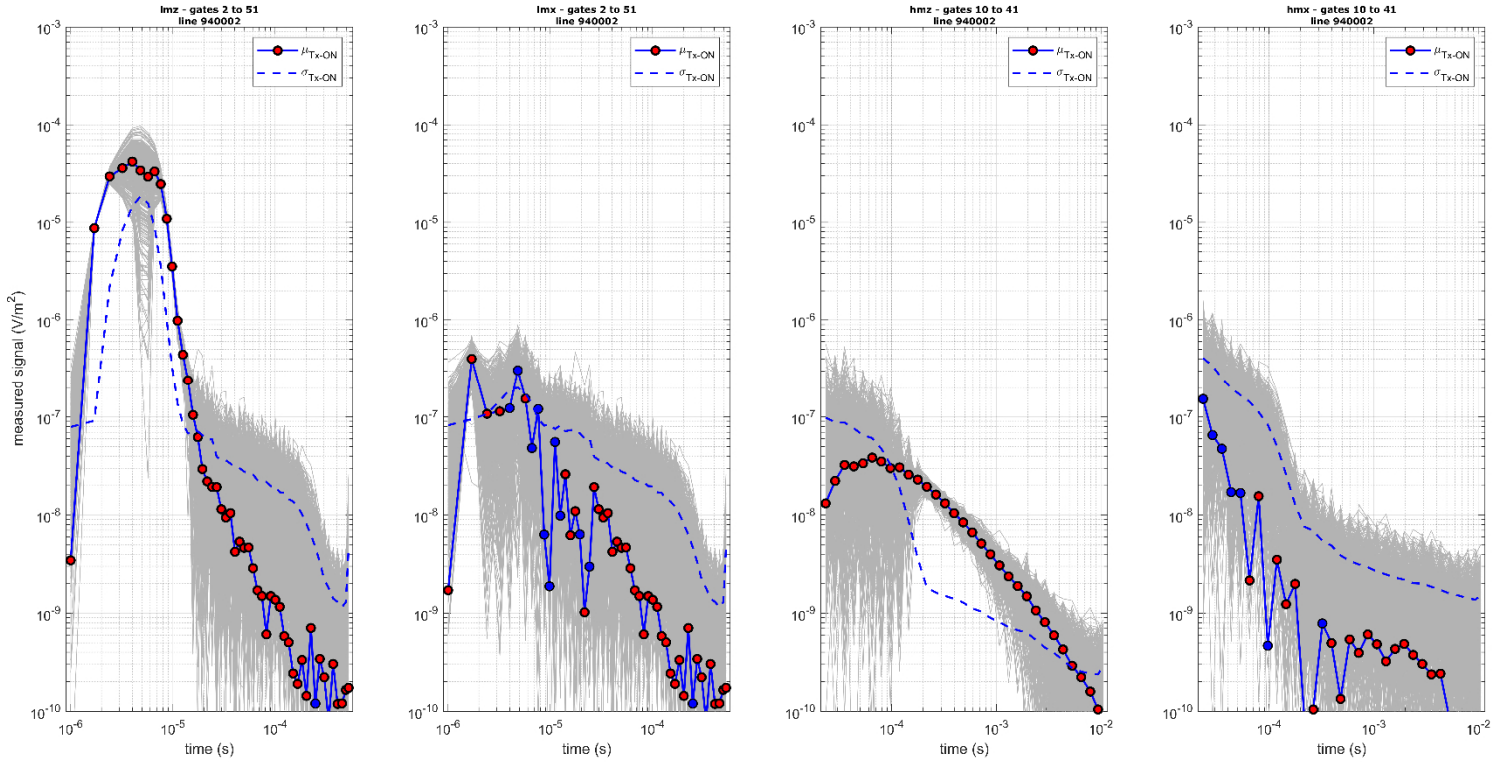

Figure 8 SkyTEM306HP high altitude data from flight 20220812.01. From left to right the four panels show LM Z uncorrected data, LM Z PFC corrected data, HM Z data, and HM X data.

Magnetic tests

The magnetic lag test was flown on August 10th, and heading test were flown on August 27th, 2022.

Magnetic lag test

The magnetic lag test was carried out by flying 2 passes perpendicular over a magnetic anomaly in form of a railroad (Figure 9). The test was conducted in flight 20220810.02 in the Limoges block of the survey campaign. The processed data includes a shift in the location of the raw magnetic data reflecting the time taken for the magnetic field measured by the airborne magnetometer to be moved to the centre of the frame. The test showed a lag of -0.2 sec in the magnetometer system. The anomaly along the test lines is seen in the images on Figure 10 along with the magnetic response.

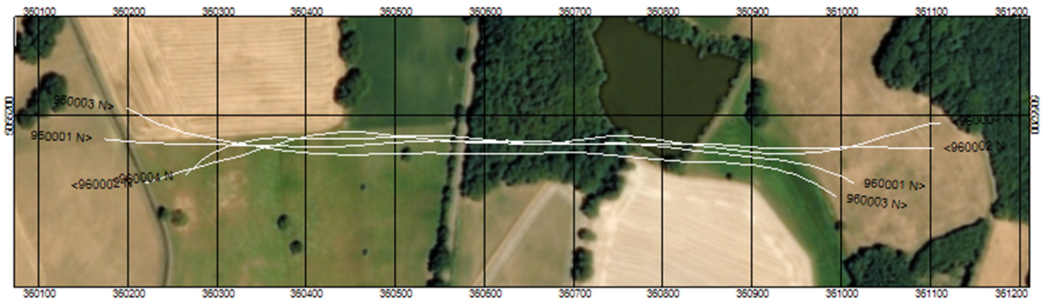

Figure 9 Location of lag test flown on 20220810.02

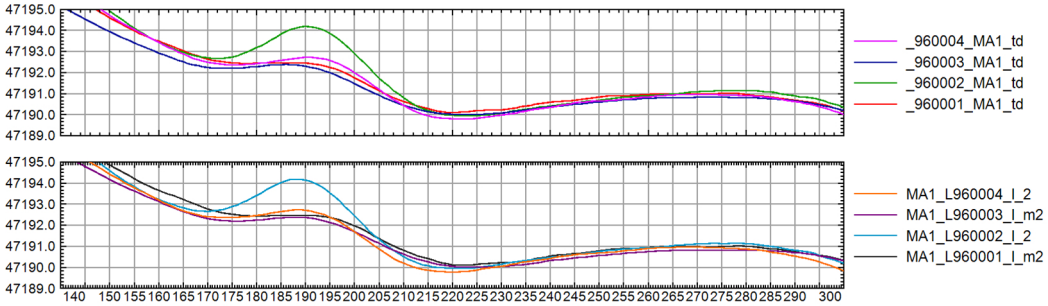

Figure 10 Lag test from flight 20220810.02. The upper panel show the original magnetic data and the lower panel show the magnetic data with a lag shift of -0.2 sec.

Magnetic heading test

The magnetic heading effect is determined by surveying in a clover leaf pattern in high altitude. Two passes in each four cardinal directions were flown to estimate the heading effect. The heading test was flown on flight 20220827.02 with the SkyTEM306HPM system in the Castres block of the survey campaign (Figure 11).

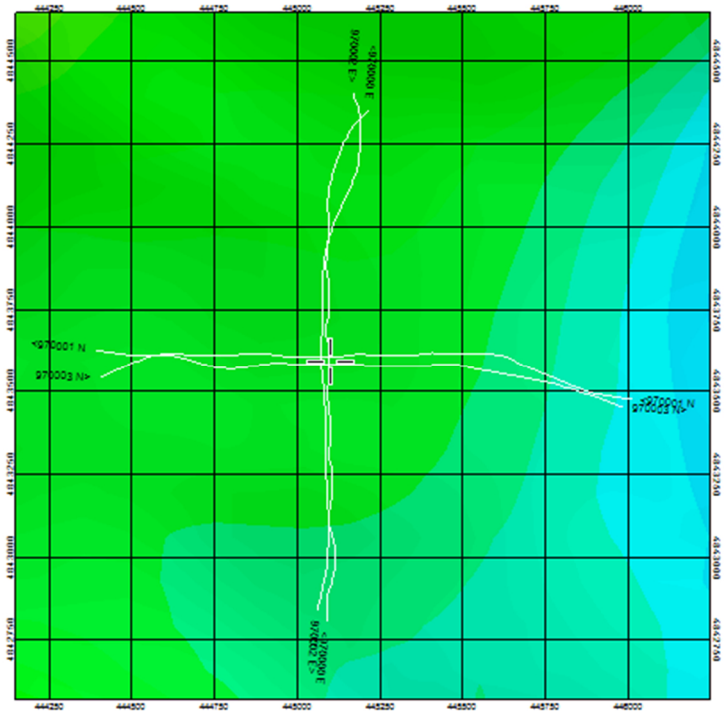

Figure 11 Location of the heading test from flight 20220827.02 on a background map of the magnetic field.

The magnetic heading test produced the heading corrections listed in Table 15. The heading corrections are less than +/- 1 nT and considered to be negligible.

Direction	Lines	**TMI (nT)**	**Heading correction (nT)**
0	970000	45882.900	0.150
90	970003	45882.800	0.050
180	970002	45882.800	0.050
270	970001	45882.500	-0.250

Table 15 Heading correction table.

Digital Data

The complete dataset of the SkyTEM survey is delivered as a Geosoft database (GDB) which can be used as input for further processing, gridding and as input to inversion and interpretation software. The channels of the GDB and xyz are described in Table 16.

Channel description, Survey Data

Parameter	Explanation	Unit
Fid	Unique Fiducial number	seconds
Line	Line number	LLLLLL
Flight	Name of flight	yyyymmdd.ff
DateTime	DateTime format	Decimal days
Date	Date	Yyyy/mm/dd
Time	Time	HH:MM:SS.ss
AngleX	Angle in flight direction	Degrees
AngleY	Angle perpendicular to flight direction	Degrees
Height	Filtered transmitter terrain clearance	Meters
Lon*	Latitude/Longitude, WGS84	Decimal degrees
Lat*	Latitude/Longitude, WGS84	Decimal degrees
E	UTM zone 31N (WGS84)	Meter
N	UTM zone 31N (WGS84)	Meter
DEM	Digital Elevation Model	Meters above sea level
Alt	DGPS Altitude	Meters above sea level
GdSpeed	Ground Speed	kph
LMcurrent	Current, low moment	Amps
HMcurrent	Current, high moment	Amps
LM_Z_dBdt[xx]**	Geosoft array channels normalized LM dB/dt Z-coil value. Voltage/(Tx moment*RX area), normalization incudes the number of transmitter turns	pV/(m4*A)
LM_Z_dBdt_MG[xx]**	Geosoft array channels normalized LM dB/dt Z-coil value for the merged LM gates. Voltage/(Tx moment*RX area), normalization incudes the number of transmitter turns	pV/(m4*A)

Parameter	Explanation	Unit
HM_Z_dBdt[xx]**	Geosoft array channels normalized HM dB/dt Z-coil value. Voltage/(Tx moment*RX area), normalization incudes the number of transmitter turns	pV/(m4*A)
HM_X_dBdt[xx]**	Geosoft array channels normalized dB/dt HM X-coil value. Voltage/(Tx moment*RX area), normalization incudes the number of transmitter turns	pV/(m4*A)
RelUnc_LM_Z_dBdt[**]	Relative uncertainty of LM_Z	-
RelUnc_LM_Z_dBdt_MG[**]	Relative uncertainty of LM_Z merged gates	-
RelUnc_HM_Z_dBdt[**]	Relative uncertainty of HM_Z	-
RelUnc_HM_X_dBdt[**]	Relative uncertainty of HM_X	-
HM_Z_B[xx]**	Geosoft array channels normalized HM Z B-field value. Voltage/(Tx moment*RX area), normalization incudes the number of transmitter turns	fT/(m2*A)
HM_X_B[xx]**	Geosoft array channels normalized HM X B-field value. Voltage/(Tx moment*RX area), normalization incudes the number of transmitter turns	fT/(m2*A)
PLNI	Powerline Noise intensity (50Hz)	PLNI
Bmag_raw	Total Magnetic Intensity (1 Hz) Magnetic base station data	nT
Diurnal	Diurnal variation Magnetic base station data	nT
Mag_Raw	Total Magnetic Intensity Raw magnetic data	nT
Mag_Cor	Magnetic Intensity Filtered and diurnal corrected	nT
RMF	Residual magnetic Field Final corrected data	nT
TMI	Total Magnetic Intensity IGRF recalculated	nT

Table 16 Channel description, survey data

**) Data positions refer to the center of the frame.*
***) The first valid gates are: Gate 4 (LM) and Gate 6 (HM).*

Inversion results

The result of the spatially constrained inversion (SCI) is delivered as a Geosoft database (GDB) and xyz ascii-file containing the modelled layer resistivity's. The channels of the GDB and xyz are described in Table 17.

The applied gridding methods, cell size, blanking distance and filtering are listed in Table 18.

Channel description, EM inversion database

Parameter	Explanation	Unit
Line	Line number	LLLLLL
E	UTM Zone31N (WGS84)	Meter
N	UTM Zone31N (WGS84)	Meter
DTM	Digital Terrain Model	Meters above mean sea level
ResI1	Residual of data	-
Height	Filtered Height Measurement	Meter
InvHei	Inverted Height	Meter
DOI	Depth of Investigation	Meter
DOI_elevation	Depth of Investigation	Depth below terrain
Res_doi_array [xx]	Conductivity of layer xx Masked below DOI	Ohmm
Res_array [xx]	resistivity of layer xx	Ohmm
Elev_array[xx]	Elevation of top of layer xx	Meter
RUnc_array[xx]	Relative uncertainty of layer xx	-

Table 17 Channel description, inversion results

Gridding method and parameters

Area	Gridding algorithm	Gridding filter	Cell size	Blanking distance
Limoges	Minimum curvature	-	133 m	400 m

Table 18: Geosoft gridding

Data processing and presentation

This section covers processing of auxiliary data, magnetic data, processing and inversion of EM data and presentations.

All devices (DGPS, Laser altimeters, inclinometers) are moved to the centre of the frame and corrected for the tilt of the frame hence all data positions refer to the center of the frame. Data is split at the beginning and end of each planned flight line.

After the initial filtering all data are resampled to 10Hz.

Auxiliary data

Tilt processing

The X and Y angle processing involves manual and automated routines using a combination of the SkyTEM in-house software SkyLab and Geosoft.
The processing involves the following steps:

- 3 sec box filter (SkyLab)
- Low pass filtering of 3.0 sec. (Geosoft)

Height processing

The height processing involves automated routines using a combination of the SkyTEM in-house software (HEfiltering and SkyLab) and Geosoft.
The processing involves the following steps:

1. Iterative weighted splines to remove low values to correct for the canopy effect (treetop filter) (HEfilter)
2. Final spline of remaining data (HEfilter)
3. Tilt correction (SkyLab)
4. Averaging of the two laser values (SkyLab)
5. Additional filters:
    a. Low pass filter of 3.0 sec (Geosoft)

DGPS processing

The DGPS has been PPP processed (Precise Point Positioning) using the Waypoint GrafNav Differential GPS processing tool. The standard airborne settings have been used.

- Import of airborne files (Rover)
- Download precise ephemeris and almanac
- Precise Point Positioning
- Export solution as .txt file

The DGPS.txt files are used as input to the SkyLab software assuring DGPS corrected data in the processed files.

The ground speed, altitude, latitude and longitude from the processed DGPS' are imported into Geosoft and merged into the final database where the coordinates are converted into UTM Zone31N (WGS84) and a low pass filter of 3.0 sec is applied.

Digital elevation model

A digital elevation model (DEM) has been calculated by subtracting the filtered laser altimeter data from the DGPS elevation. All steps related to the DEM are carried out Geosoft.
The processing of the final DEM involves the following steps:

- Filtering and processing of the laser altimeter height as described above
- DEM data received by subtraction of final filtered laser data from final processed DGPS altitude data

Figure 12 shows the DEM.

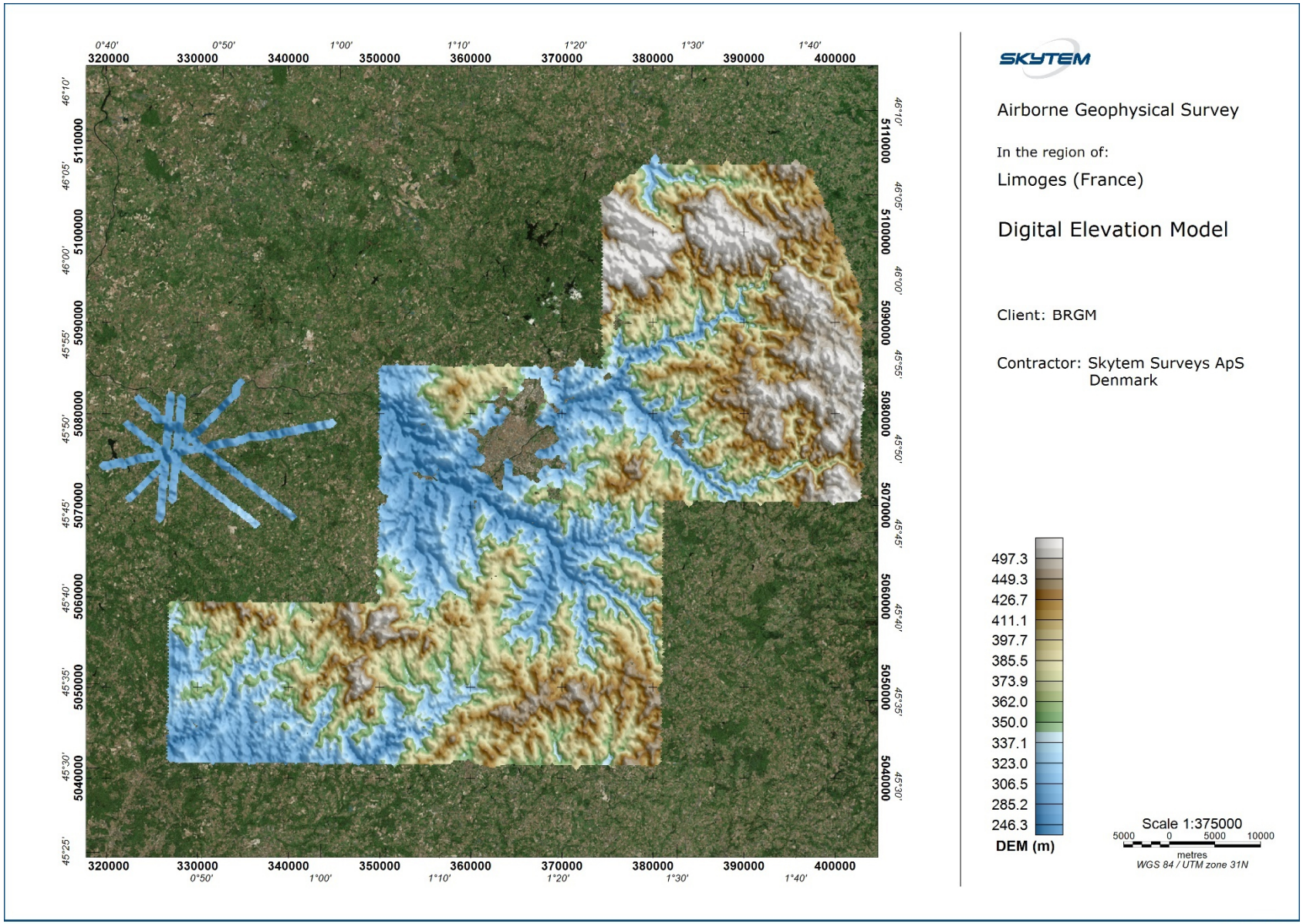

Figure 12. DEM.

Magnetic data

Final processing of the magnetic data involves the application of traditional corrections to compensate for diurnal variation effects. Geosoft magnetic data processing tools are applied as follows:

- Processing of static magnetic data acquired on magnetic base station
- Pre-processing of airborne magnetic data
    - Stacking of data to 10 Hz in SkyLab.
    - Moving positions to the center of the system in SkyLab.
- Processing and filtering of airborne magnetic data
- Standard corrections to compensate the diurnal variation
- IGRF correction
- Gridding

Processing of base station magnetic data

The base station magnetometer data was merged into the base station Geosoft database daily for further processing.

The following filtering was applied:

- Fraser Low-pass filter (width 60 sec)
- The overall average (Limoges: 47081.1 nT, Nexon: 47045.1 nT) of the residual field of the base station data was subtracted to calculate the diurnal.

Processed diurnal magnetic data from the magnetic base station representing short term variations was merged with airborne magnetic data.

Processing and Filtering of airborne magnetic data

Airborne magnetic data is filtered and interpolated as follows:

- Adjustment of the data for the time lag between the GPS position and the position of the magnetic sensor
- Data resampling to 10 Hz (stacking)
- Manual despiking to remove spikes and spurious data
- Geosoft processing:
    - Interpolation (Akima)
    - LP filter (3 sec)

Corrections to the magnetic data

The following corrections are applied to the airborne magnetic data:

- Correction for diurnal variation using the digitally recorded ground base station magnetic values as described above
- Lag of -0.2 sec (two fid=0.2 sec) was applied
- Heading was negligible and no correction was applied
- IGRF correction
- No removal of cultural effects has been applied

IGRF correction

The International Geomagnetic Reference Field (IGRF) is a long-wavelength regional magnetic field calculated from permanent observatory data collected around the world. The IGRF is updated and determined by an international committee of geophysicists every 5 years. Secular variations in the Earth's magnetic field are incorporated into the determination of the IGRF.

The IGRF model is calculated before levelling using the following parameters:

- IGRF model year: 2020
- Date: variable according to date channel in database
- Position: variable according to GPS WGS84 longitude and latitude
- Elevation: variable according to magnetic sensor altitude derived from DGPS data

Micro-levelling of magnetic data

After applying the above corrections to the magnetic data micro-levelling was applied as a standard procedure.

Microlevelling:

- Decorrugation cutoff wavelength = 2000 m
- Naudy filter length = 2000 m

The calculated corrections were subtracted from the Mag data.

RMF and TMI recalculation

The outcome of processed magnetic data after all corrections and levelling is the Residual Magnetic Field (RMF).

Total magnetic intensity (TMI) is recalculated to an average altitude by adding the IGRF regional field back to RMF on a fixed date (2022/07/20) and fixed altitude (438 m) for each individual point.

Figure 13 show the Residual Magnetic Field map.

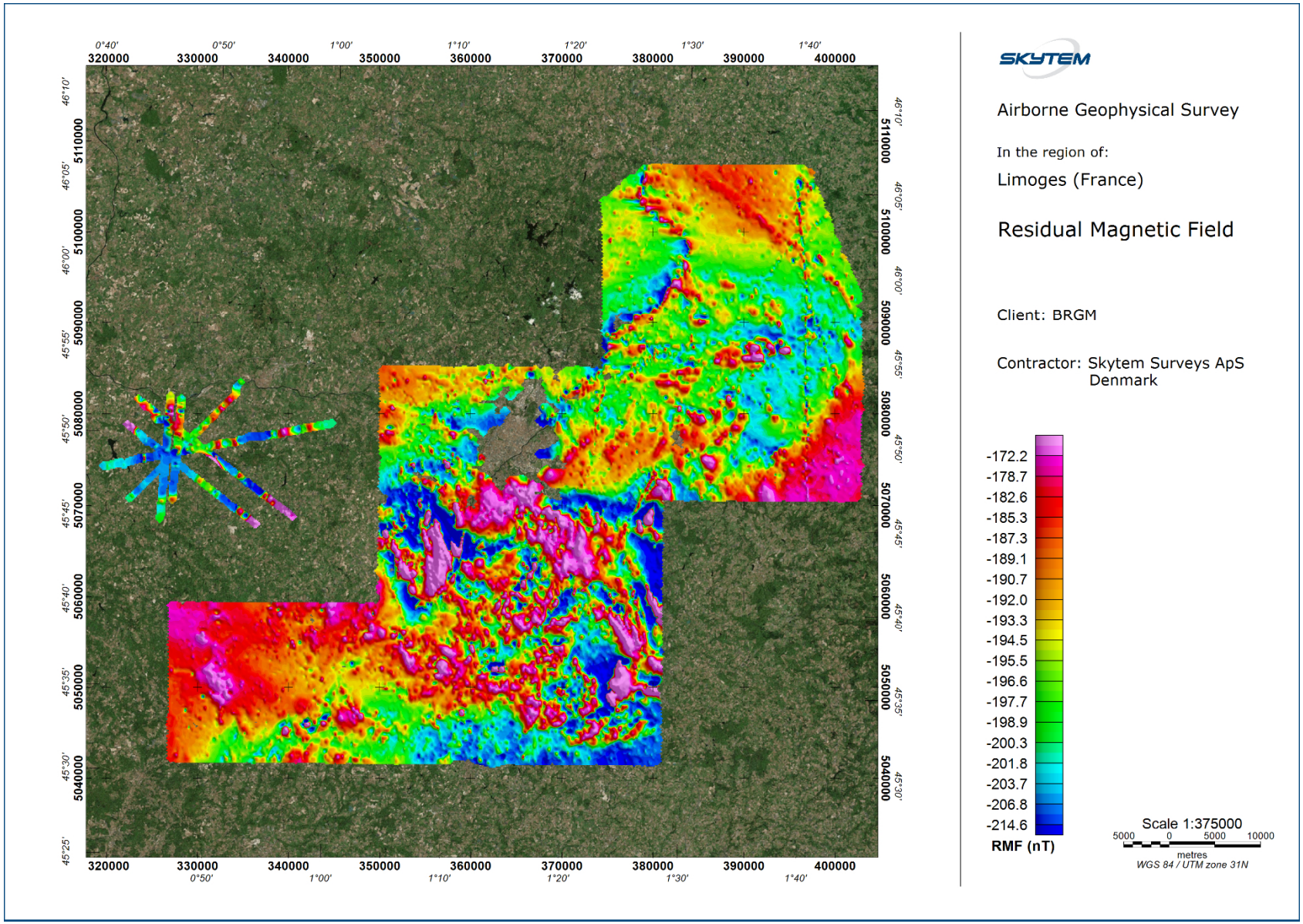

Figure 13. Residual Magnetic Field.

EM data

This section covers processing of EM data and filtering of EM data.

Primary Field Compensation (PFC)

The magnetic field coupling between the receiver coils and the transmitter loop is continuously hardware-monitored, providing a separate value for the magnetic field coupling during each transient sounding. These data are used for raw data correction in a separate post-processing step. The primary field compensation technique has proven stable and has routinely yielded a reduction of the primary field influence in very early time gates by a factor exceeding 50.

EM Filtering

The data are normalized in respect to effective Rx coil area, Tx coil area, number of turns and current giving the unit [pV/(m^4*A)].

Pre-averaging steps

Prior to applying standard averaging to the recorded data, the raw data are subjected to a few data processing steps:

- PFC correction of LM Z dBdt SkyTEM306HPM system
- Outlier rejection filtering of the raw data, which reduces the influence from spherics and transient cultural noise. Outlier rejection has been performed on a gate-by-gate basis as a non-linear STD-estimate-scaled thresholding and interpolation process on minimally averaged EM data. The thresholding is a variant of the Median Absolute Deviaiton outlier detection method.
- Removal of constant system self-response (bias) on SkyTEM306HPM HM and dBdt and B-field data
- Estimation of noise standard-deviation throughout the survey area on a gate-by-gate basis

The level of the constant system self-response (bias) is found in high altitude, where the recorded signal is free of signal from the ground. The self-response is approximated by fitting a sum of exponential functions to the sounding curves and subsequently the self-response is removed from data by subtracting the approximation. The system self-response values are listed in Table 19.

Gate / Channel	HM Z dBdt spline V/m²	HM X dBdt spline V/m²	HM Z B-field nT	HM X B-field nT
1	-	-	-	-
2	-	-	-	-
3	-	-	-	-
4	-	-	-	-
5	-	-	-	-
6	-	-	-	-
7	-6.523139E-08	-5.358164E-07	1.636786E-11	-1.722714E-12
8	-3.766861E-08	-3.753032E-07	1.650262E-11	-4.088854E-13
9	-1.350354E-08	-2.436010E-07	1.656127E-11	5.554436E-13
10	6.052263E-09	-1.447668E-07	1.654083E-11	1.292199E-12
11	2.062411E-08	-7.687036E-08	1.642847E-11	1.770589E-12
12	3.023922E-08	-3.530884E-08	1.621597E-11	2.046774E-12
13	3.538592E-08	-1.355418E-08	1.591434E-11	2.175205E-12
14	3.712895E-08	-3.970229E-09	1.552875E-11	2.222627E-12
15	3.660297E-08	-5.808108E-10	1.505863E-11	2.232442E-12
16	3.476167E-08	3.437398E-10	1.451293E-11	2.227729E-12
17	3.221579E-08	5.255053E-10	1.389567E-11	2.217866E-12
18	2.928403E-08	5.475251E-10	1.320920E-11	2.205173E-12
19	2.611456E-08	5.462741E-10	1.245826E-11	2.189649E-12
20	2.281699E-08	5.423322E-10	1.165286E-11	2.170761E-12
21	1.949404E-08	5.374359E-10	1.081643E-11	2.148059E-12
22	1.627622E-08	5.315189E-10	9.957202E-12	2.120494E-12
23	1.328822E-08	5.243822E-10	9.102213E-12	2.087409E-12
24	1.063805E-08	5.157908E-10	8.261900E-12	2.047518E-12
25	8.398046E-09	5.054928E-10	7.451707E-12	1.999797E-12
26	6.580785E-09	4.931922E-10	6.676292E-12	1.942928E-12
27	5.146914E-09	4.785761E-10	5.935786E-12	1.875516E-12
28	4.022635E-09	4.613101E-10	5.228293E-12	1.796039E-12
29	3.131410E-09	4.410679E-10	4.555229E-12	1.703140E-12
30	2.416433E-09	4.175383E-10	3.920669E-12	1.595696E-12
31	1.846390E-09	3.904973E-10	3.327243E-12	1.472657E-12
32	1.402552E-09	3.598341E-10	2.776891E-12	1.334049E-12
33	1.065272E-09	3.256270E-10	2.266328E-12	1.180521E-12
34	8.094272E-10	2.882290E-10	1.792440E-12	1.014157E-12
35	6.092458E-10	2.483267E-10	1.355994E-12	8.385545E-13
36	4.457830E-10	2.070072E-10	9.644909E-13	6.591327E-13
37	3.100216E-10	1.657469E-10	6.299573E-13	4.829200E-13
38	2.004546E-10	1.263376E-10	3.635400E-13	3.179584E-13
39	1.179560E-10	9.068067E-11	1.700860E-13	1.724041E-13
40	6.843929E-11	6.449947E-11	4.480392E-14	5.288571E-14
41	4.463234E-11	4.935749E-11	0	0

Table 19: System self-response values

Averaging approach

The averaging approach comprises applying a tapered convolution filter to all gates, where the filter has a fixed duration independent of the gate number. The full width at half maximum of the applied filter is 2.0 s.

Height correction to a common flight altitude has been applied to the Z component EM data and are provided in HeightCor grids. A flight altitude of 50 m was applied to the SkyTEM306HPM.

Figure 14 and Figure 15 show examples of Low and High Moment height corrected data from the SkyTEM306HPM system.

A complete set of grids and maps can be found in the data delivery folder.

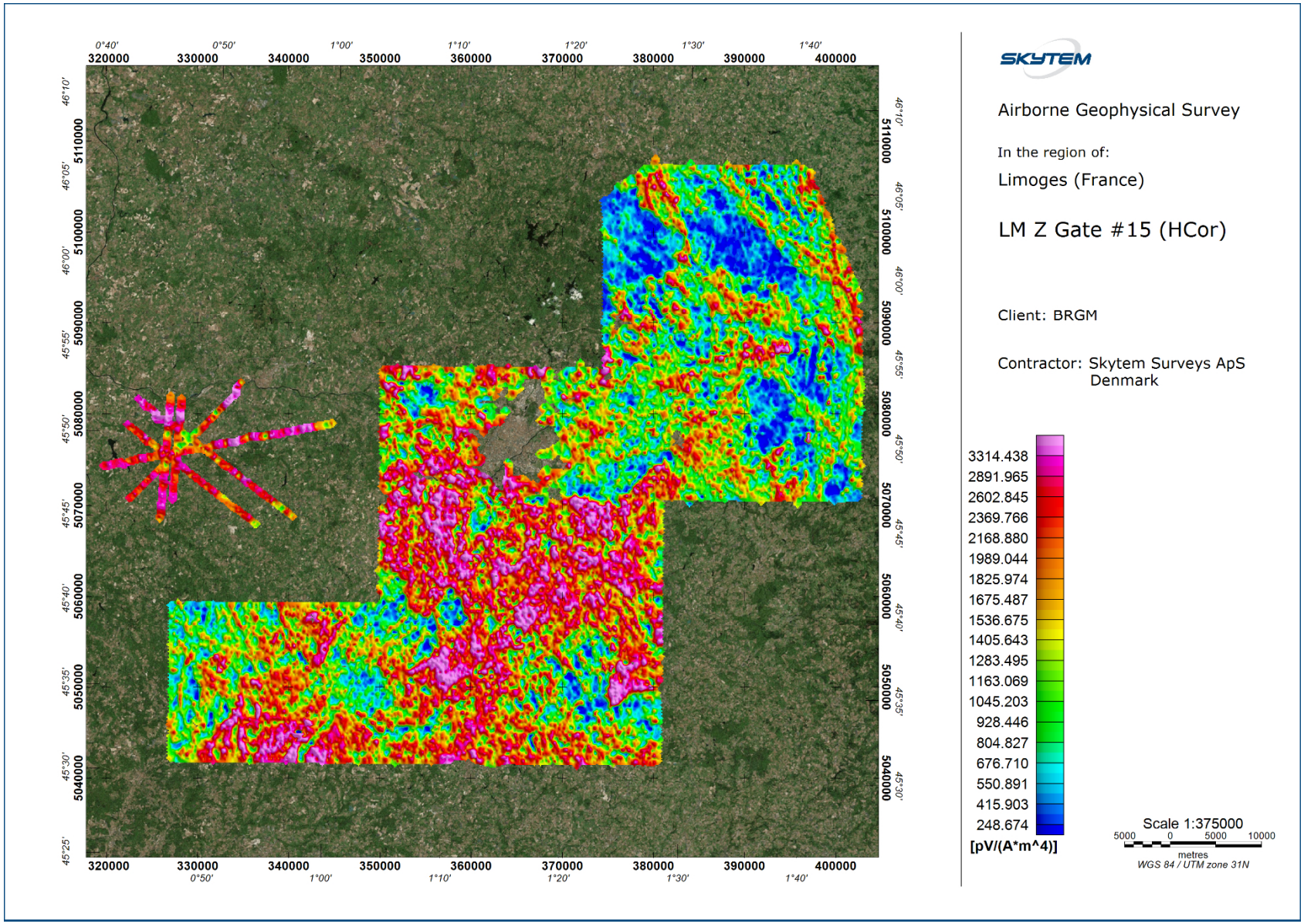

Figure 14. SkyTEM306HPM height corrected low moment Z dB/dt gate 15.

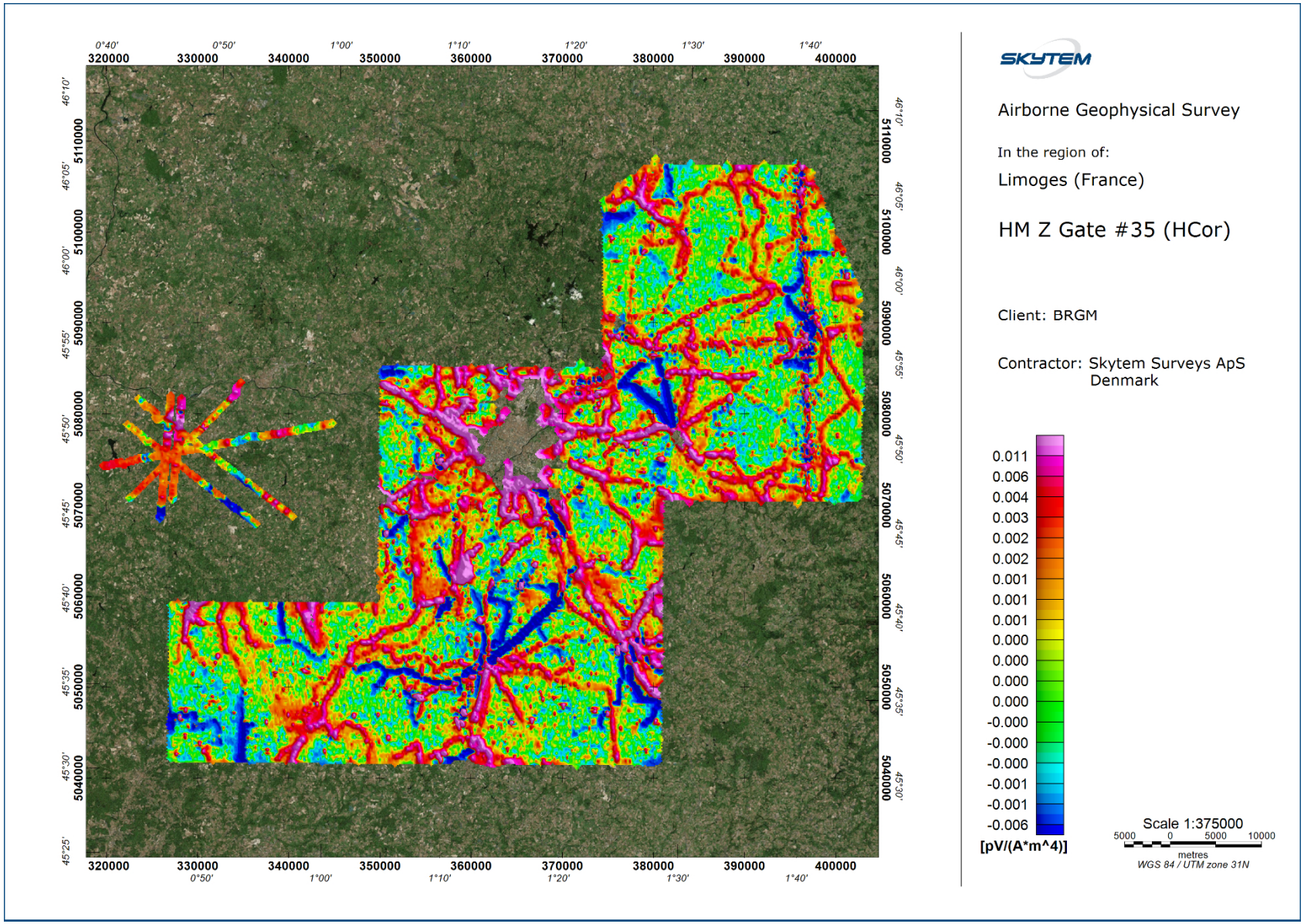

Figure 15. SkyTEM306HPM height corrected high moment Z dB/dt gate 35.

B-field

The B-field data are recorded using the same induction coil receivers as are used for the dB/dt data. The receivers continuously monitor all B-field changes in their respective field component over the entire waveform (i.e. both during ON- and OFF time).

The continuous monitoring and the ability to integrate these changes allows for exact measured B-field response outputs.

Notice that the periodic and sign-alternating properties of the transmitted waveform permits the unique and accurate determination of the constant of integration.

Figure 16 show an example of a B-Field gate for the SkyTEM306HPM system. All other gates are found in the data delivery folder.

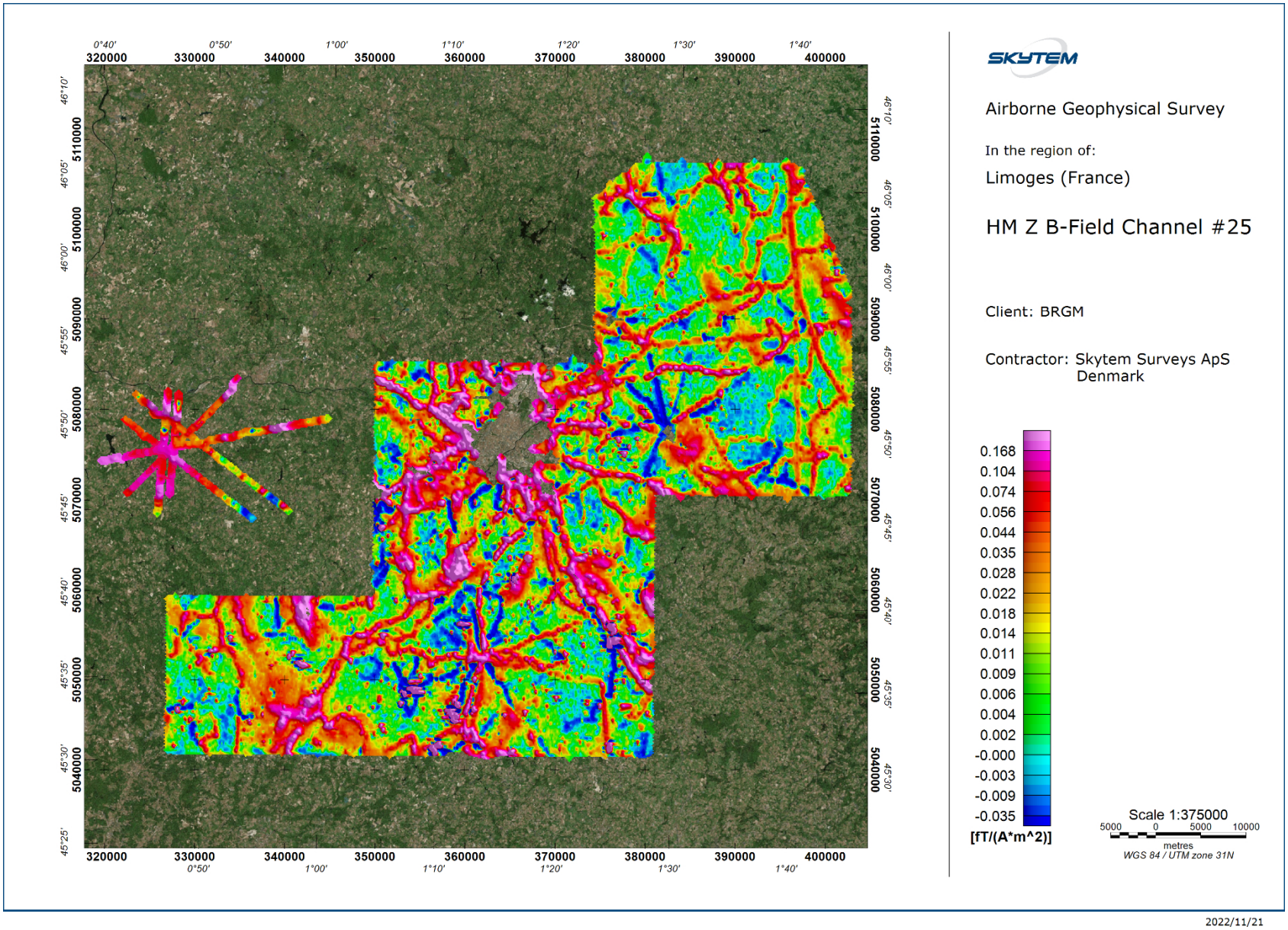

Figure 16. SkyTEM306HPM High Moment Z B field channel 25.

Power Line Noise Intensity (PLNI)

The PLNI is a powerful tool for identifying power line noise effect on EM and magnetic data. The PLNI monitor values are derived from a frequency analysis of the raw Z-component EM data. The Fourier transformation is evaluated at the local power transmission frequency yielding the amplitude spectral density of the power line noise.

CAUTION - When evaluating the PLNI values one should be aware of the following factors that may give rise to anomalous PLNI patterns unrelated to the actual power line noise level:

- Other noise sources than power line noise may contribute to the total noise spectral density in the data at the power transmission frequency. When power line noise is present it tends to dominate all such other noise sources.
- The presented PLNI values are not corrected for fly height or frame angles, which means that adjacent lines crossing the same power line may not exhibit the same values of PLNI.

Figure 17 shows the PLNI.

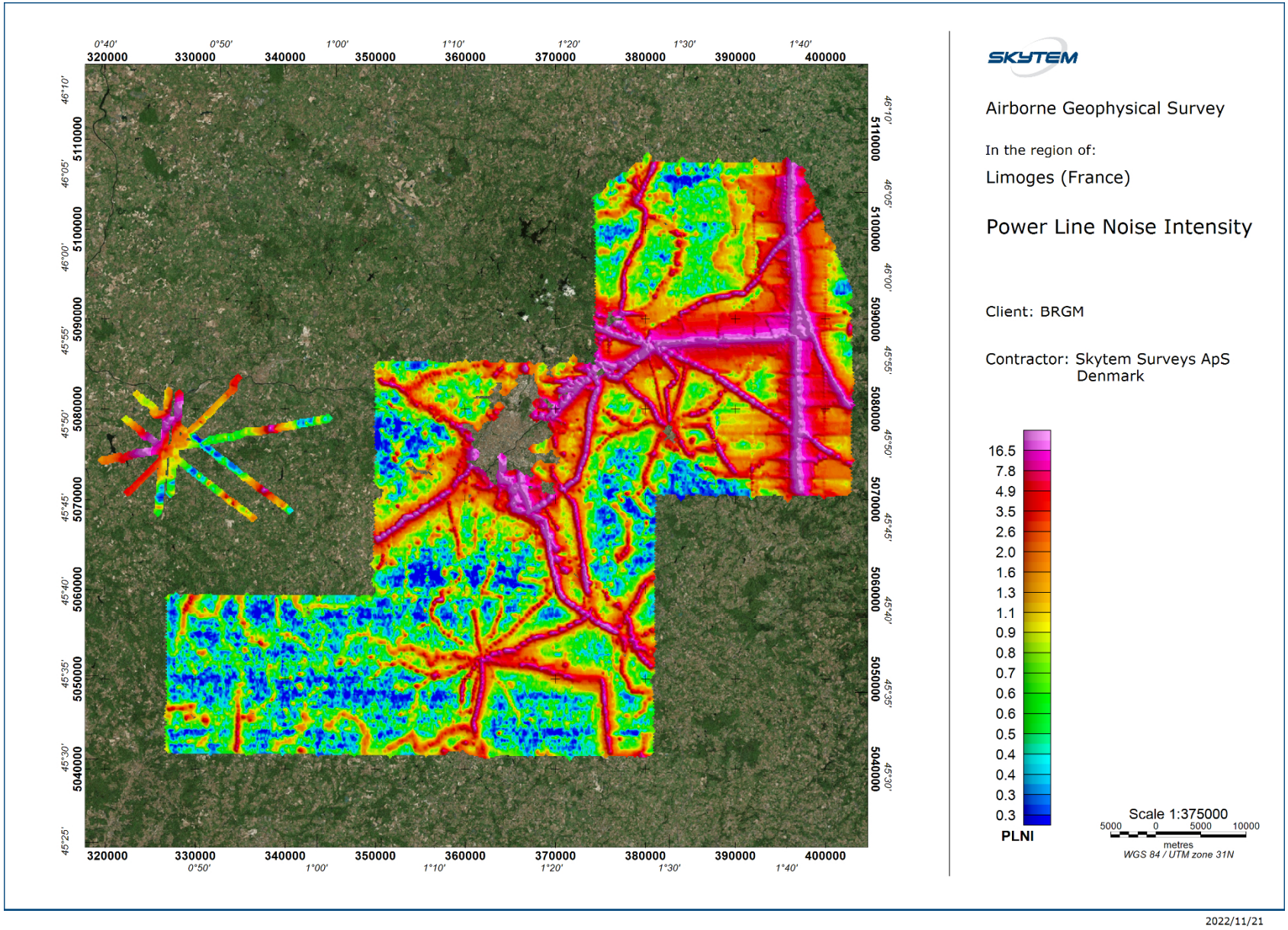

Figure 17. Power line noise intensity

Adaptive Time Constant (TAU)

An adaptive Tau calculation has been performed on HMZ data.

The adaptive Tau method treats each sounding curve individually and involves the following steps for each sounding position:

- Identifying the latest gate with a relative data uncertainty below a user-defined threshold. Later gates are regarded as having too low S/N ratio to be reliably used in the subsequent fitting operation.
- Fitting an exponential function to a user-defined number of consecutive gates up to and including the latest gate defined above. The fitting procedure follows the latter formulation given in (1) using end-of-ramp referenced gate times.

For the present survey following parameters were applied:

SkyTEM306HPM:

Upper threshold for acceptable relative uncertainty	0.30
Consecutive gates used in each exponential fit	5

In addition to a map of adaptive tau values, Figure 18, a grid of latest gate used for the exponential fit are made and can be found in the digital data delivery.

---

(1) Weisstein, Eric W. "Least Squares Fitting--Exponential." From MathWorld--A Wolfram Web Resource. http://mathworld.wolfram.com/LeastSquaresFittingExponential.html

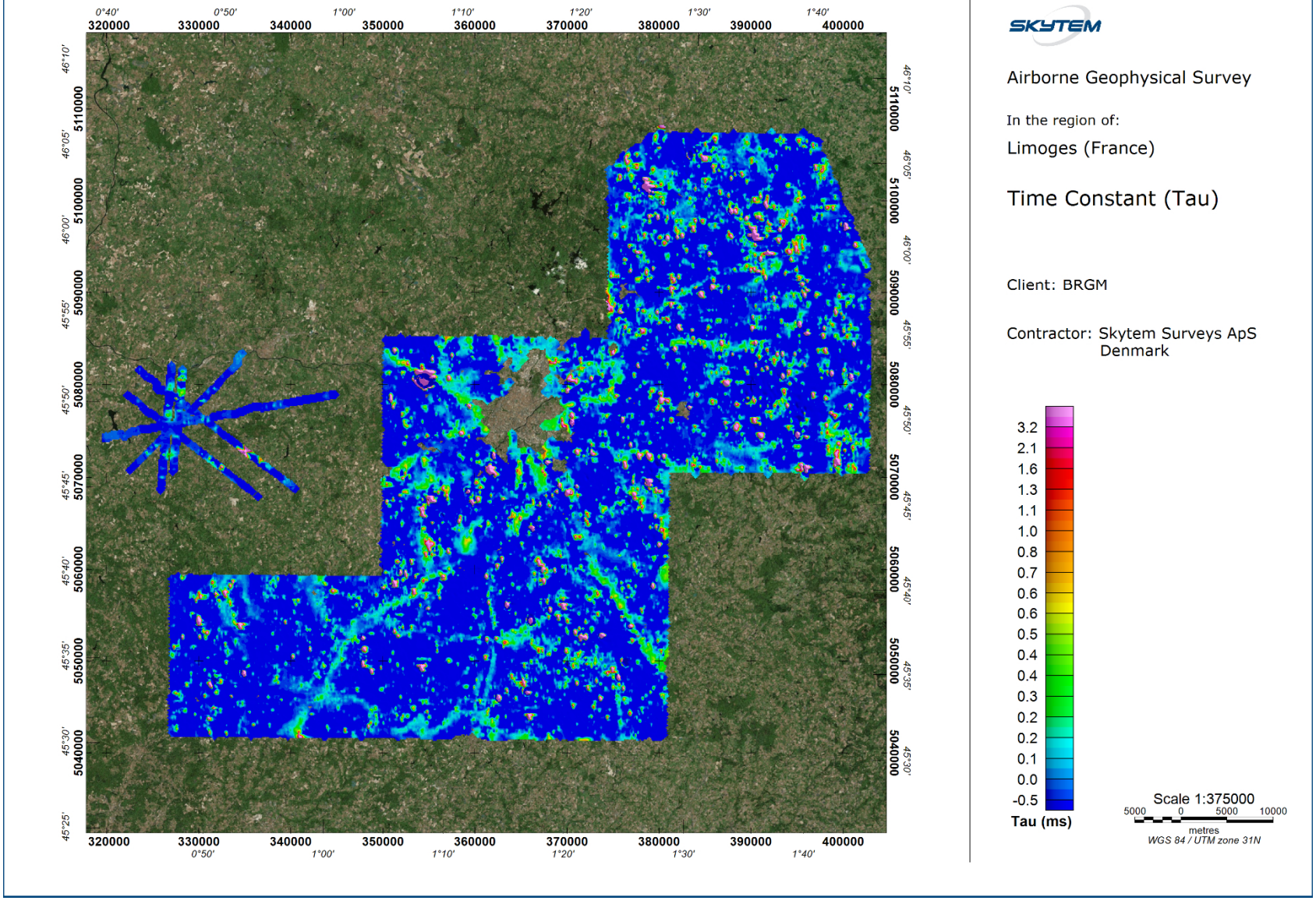

Figure 18 SkyTEM306HPM system. Adaptive Tau. Calculation based on 5 last gate values with a relative uncertainty less than 0.30

Inversion

In this section, the particulars of modelling and inversion of SkyTEM data near Limoges will be described.

The SkyTEM data have been processed and inverted using spatially constrained inversion (SCI) in Aarhus Workbench, a unique software package initially developed at Aarhus University, Denmark. In this SCI algorithm a group of time-domain EM (TEM) soundings are inverted simultaneously using 1-D models. Each sounding yields a separate layered model, but the models are constrained laterally. See Figure 19.

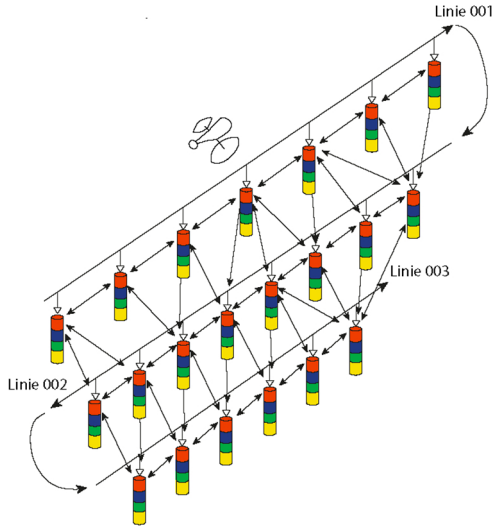

Figure 19. Schematic presentation of the SCI setup. Constraints connect not only soundings located along the flight line, but also those across them (figure from hgg.au.dk).

Initial model and optimisation norm

The SCI code is run in multi-layer, smooth-model mode in which the layer thicknesses are fixed, and the data are inverted only for resistivity.

In the inversion of the SkyTEM306HPM system the thickness of the first layer is set to 3 m and the depth to the top of the deepest layer boundary is 500 m.

When computing the layer thicknesses, the first and last layer boundary scales the model thicknesses automatically using a log distribution. Thicknesses and depths to the top of each layer for the current project are given in Table 20 for the SkyTEM306HPM.

The input data to the inversion are the LM merged gates and HM dB/dt Z-component EM data. The initial model resistivity structure is a homogenous half-space model with an 500 ohmm starting resistivity.

Gates 1 to 10 from the LM and gates 1 to 7 form the HM has been omitted from the inversion. Prior to the inversion EM data with relative uncertainties higher than 0.40 have been masked.

Manually masking of data displaying coupling effects e.g. due to power lines is not part of the current project and therefore cultural effects in the EM data can be present in the final data base.

Layer #	Layer Thickness [m]	Depth to top of layer [m]
1	3.0	0.0
2	3.3	3.0
3	3.7	6.3
4	4.1	10.0
5	4.5	14.1
6	5.0	18.5
7	5.5	23.5
8	6.1	29.0
9	6.7	35.1
10	7.4	41.8
11	8.2	49.3
12	9.1	57.5
13	10.1	66.6
14	11.2	76.7
15	12.3	87.9
16	13.7	100.2
17	15.1	113.9
18	16.7	129.0
19	18.5	145.7
20	20.4	164.1
21	22.6	184.6
22	25.0	207.2
23	27.7	232.2
24	30.6	259.9
25	33.9	290.5
26	37.5	324.4
27	41.5	361.9
28	45.9	403.4
29	50.8	449.3
30	-	500.0

Table 20 SkyTEM306HPM system. Layer distribution of the multi-layer smooth inversion model

Model Presentation - Model sections and maps

The models resulting from the inversion are presented as layer resistivity profiles, grids, and maps of mean resistivity in depth intervals in Geosoft and pdf format. Figure 20 show an example of a layer resistivity profile from the SkyTEM306HPM, and Figure 21 show an example of the map resistivity layer from SkyTEM306HPM. All profiles, grids, images, and maps are included in the digital data delivery.

Model Sections

The profile plots consist of four sections; the top section shows the inverted models, with topography, where the resistivity of the individual layers is colour coded according to the colour bar. The resistivity is shown on a logarithmic scale and conductive and resistive features appear with the same weight. The thin grey line indicates the upper DOI. The white shading in the analysis section indicates the estimated depth of investigation (DOI). Where the colour fades into the white, the inverted resistivity is determined almost exclusively by the regularization, i.e. the resistivity is essentially undetermined. The measured and inverted flight elevation is shown with a black and blue line, respectively, above the model section.

The second and the third section show the measured data (dots) together with the response of the inverted models (solid lines) for low moment data (LMZ) and high moment data (HMZ). Blank sections in the profile indicate areas where the data falls for an inversion setting criteria, e.g. the signal to noise ratio has been too low for any data to be used in the inversion. Essentially the resistivity in those sections can be considered as "Very high" (>1000 Ωm). Alternatively, data have been negative, or a man-made conductor has interfered with the signal, which can also lead to data being discarded prior the inversion.

The bottom section shows the data residual (black dots) of the inversions.

In the section to the right, an overview map of the survey with an indication of the given line and flight direction is seen.

The quality of the inversion results can be evaluated by inspecting the residuals. The data residual is calculated by comparing the measured data with the response of the resulting model after inversion. If the residual is in the range of 1, the misfit between the response of the final model and the data is, on average, equal to the noise. If the residual is high, it might be caused by data that are noisier than the noise model takes into account. This can be seen where resistivity is very high and the signal consequently very low. A high data residual can also be due to the inconsistency between the 1D model assumed in the inversion and the 2D/3D character of the real world. These are found primarily at the edges of sharp lateral resistivity contrasts. Finally, coupling effects due to power lines and other manmade conductors can also be a source of a high residual as well as the presence of induced polarization in the EM data.

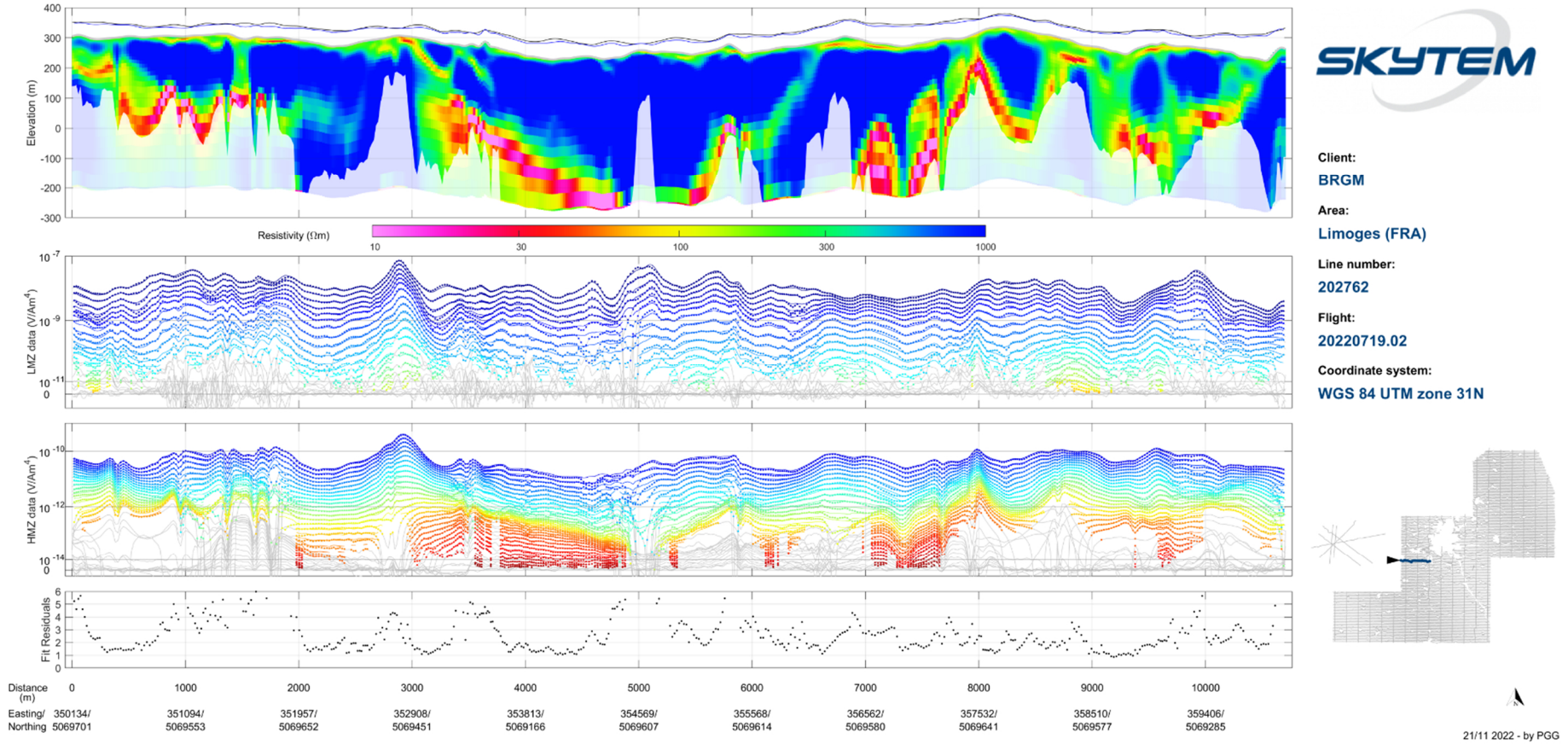

Figure 20 Example of section plot from the inversion of SkyTEM306HPM data. From top to bottom: conductivity section with flight height and Depth of Investigation (DOI), LM and HM gate plot (data=dots, model=line), residual.

Layer resistivity maps

The layer resistivity maps show the inverted resistivity for each of the model layers. As the thickness of the model layers increases downwards the maps represent a varying thickness interval. The depth intervals for each layer are stated on the maps in meters below the surface.

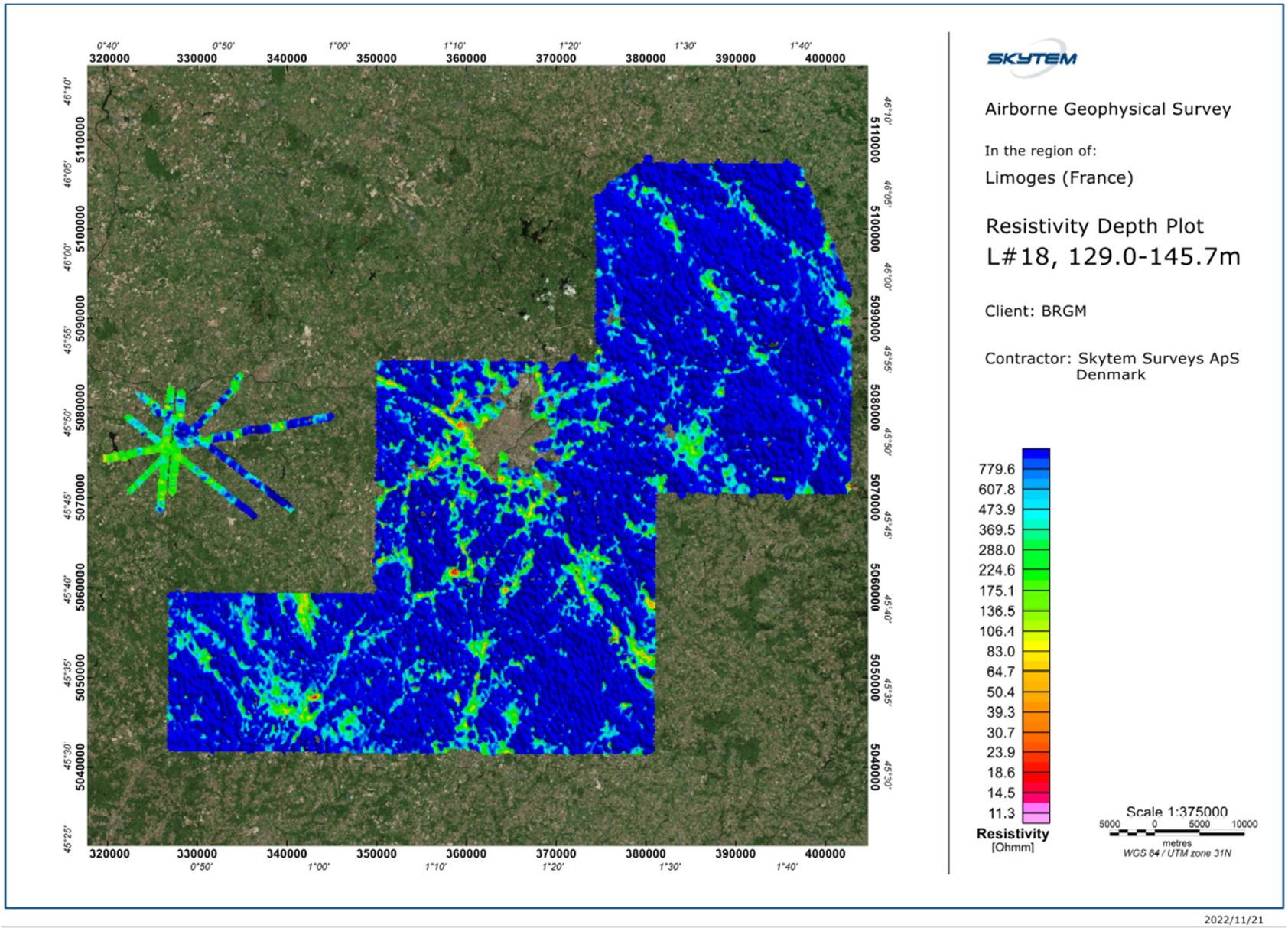

Figure 21 SkyTEM306HPM system: Modelled Layer Resistivity of layer 18 (depth 129.0 m – 145.7 m).

References

Aarhus University, n.d., Guide to 1D-LCI inversion.

Auken, E., Foged, N. and Sørensen, K., 2002, Model recognition by 1-D laterally constrained inversion of resistivity data: Proceedings – New Technologies and Research Trends Session, 8th meeting, EEGS-ES.

Auken, E., Christiansen, A. V., Jacobsen, B. H., Foged, N., and Sørensen, K. I., 2005, Piecewise 1D Laterally Constrained Inversion of resistivity data: *Geophysical Prospecting*, 53, 497–506.

Christiansen, A.V. and Auken, E., 2012, A global measure for depth of investigation: *Geophysics,* vol 77, No. 4, 171-177.

Sattel, D., 2005, Inverting airborne electromagnetic (AEM) data with Zohdy's method, Geophysics, 70, G77-G85.

Appendix list

Appendix 1: Instruments

Instrument positions

The instrumentation involves a time domain electromagnetic system, two inclinometers, two altimeters and two DGPS'.

The measurements were carried out, using a setup as described below.

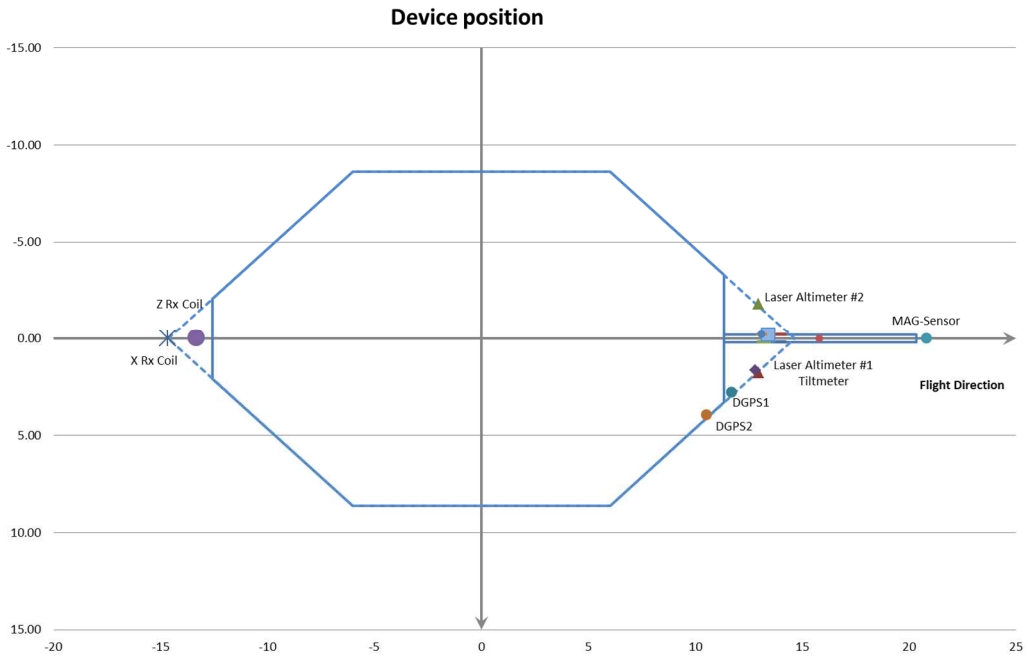

Figure 1 Sketch showing the frame and the position of the basic instruments. The blue line defines the transmitter loop. The horizontal plane is defined by (x, y).

The location of instruments in respect to the frame is shown in Figure 1 and is given in (x, y, z) coordinates in the table below.

X and y define the horizontal plane. Z is perpendicular to (x, y). X is positive in the flight direction, y is positive to the right of the flight direction, and z is positive downwards.

The generator used for powering of the transmitter is ~30 m

m below the helicopter.

Device	X	Y	Z
DGPS1 (EM)	11.68	2.79	-0.16
DGPS2 (EM)	10.51	3.95	-0.16
HE1 (altim.)	12.94	1.79	-0.12
HE2 (altim.)	12.94	-1.79	-0.12
Inclinometer 1	12.79	1.64	-0.12
Inclinometer 2	12.79	1.64	-0.12
RX (Z Coil)	-13.65	0.00	-2.00
RX (X Coil)	-14.65	0.00	0.00
Mag sensor	20.50	0.00	-0.56

For the location of instruments see Figure 1.

Transmitter

The time domain transmitter loop can be described as an octagon with the corners listed below:

X	Y
-12.55	-2.10
-6.03	-8.63
6.03	-8.63
11.34	-3.31
11.34	3.31
6.03	8.63
-6.03	8.63
-12.55	2.10

The total area of the transmitter coil defined by the corner points is 342 m² and 68.3 m in circumference.

The key parameters defining the transmitter set up are:

Low Moment

Parameter	Value
Number of transmitter turns	1
Transmitter area	342 m²
Peak current	8 Amp
Peak moment	~3,000 NIA
Multi moment repetition frequency	25 Hz
On-time	1000 µs
Off-time	549.4 µs
Duty cycle	67 %
Wave form	Sinusoidal

High Moment

Parameter	Value
Number of transmitter turns	6
Transmitter area	342 m²
Peak current	225 Amp
Peak moment	~ 500,000 NIA
Multi moment repetition frequency	25 Hz
On-time	5000 µs
Off-time	15000 µs
Duty cycle	25 %
Wave form	Square

Figure 2 The 342 m² frame in production mode.

Receiver system

The decay of the secondary magnetic field is measured using two independent active induction coils. The Z coil is the vertical component, and the X coil is the horizontal in-line component. Each coil has an effective receiver area of 325 m² (Z), 115 m² (X).

The receiver coils are placed in a null-position:

Z coil (x, y, z) = (-13.65 m, 0.0 m, -2.0 m)
X coil (x, y, z) = (-14.65 m, 0.0 m, 0.0 m)

In the null-position, the primary field is damped with a factor of 0.01 on HM and due to PFC correction, it can be neglected on LM.

Figure 3 Rudder containing the Z coil located in the top part of the tower.

The key parameters defining the receiver set up are:

Receiver parameters		
Sample rate		All decays are measured
Number of output gates		41 (HM) and 51 (LM)
Receiver coil low pass filter		202.5 kHz (Z-coil) and 341.3 kHz (X-coil)
Receiver instrument low pass filter		1 MHz
Repetition frequency	Multimoment	25 Hz 25 Hz
Front gate	LM HM	0 µs 10 µs

Receiver gate times are measured from the start of the transmitter current turn-off for the LM and from the end of the transmitter current turn-off for the HM.
A complete list describing gate open, close, and centre times are listed in table 7 – 9.

Inclination

Instrument type: Bjerre Technology

The inclination of the frame is measured with 2 independent inclinometers. The x and y angles are measured 2 times per second in both directions. The inclinometers are placed in the rear of the frame as close to the z coil as possible, see Figure 1.

The angle data are stored as x, y readings. X is parallel to the flight direction and positive when the front of the frame is above horizontal. Y is perpendicular to the flight direction and negative when the right side of the frame is above horizontal.

The angle is checked and calibrated manually within 1.0 degree by use of a level meter.

GPS airborne unit and base stations

Chipset: OEMV1-L1 14-channel rate.
Antenna: Trimble, Bullet III GPS Antenna

The DPS delivers one dataset per second. The raw coordinates are given in Latitude/Longitude, WGS84.

The uncertainty in the xyz-directions is ± 1 m after processing.
The processed GPS data is combined with the EM data in the xyz-files, giving the precise position.

DGPS parameters	
Sample rate	1 Hz
Uncertainty	± 1 m

Altimeter

Instrument type: MDL ILM300R

Two independent laser units mounted on the frame measuring the distance from the frame to the ground, see Figure 1

Each laser delivers 30 measurements per second and covers the interval from 0.2 m to approximately 200 m.

Dark surfaces including water surfaces will reduce the reflected signal. Consequently, it may occur that some measurements do not result in useful values.

The altimeter measurements are given in meters with two decimals. The uncertainty is 10 - 30 cm. The lasers are checked on a regular basis against well-defined targets.

Laser parameters	
Sample rate	30 Hz
Uncertainty	10 - 30 cm
Min/ max range	0.2 m / 200 m

Magnetometer airborne unit

Instrument type: Geometrics G822A sensor and Kroum KMAG4 counter.

The Geometrics G822A sensor and Kroum KMAG4 counter is a high sensitivity Cesium magnetometer. The basic of the sensor is a self-oscillating split-beam Cesium vapor (non-radioactive) Principle, which operates on principles similar to other alkali vapor magnetometers.

The sensitivity of the Geometrics G822A sensor and Kroum KMAG4 counter is stated as <0.0005 nT/√Hz rms. Typically 0.002 nT P-P at a 0.1 second sample rate, combined with absolute accuracy of 3 nT over its full operating range.

The magnetometer is synchronized with the TEM system. When the TEM signal is on, the counter is closed. In the TEM off-time the magnetometer data is measured from 100 microseconds until the next TEM pulse is transmitted. The data are averaged and sampled as 25 Hz.

Parameter	Value
Sample frequency	25 Hz

Magnetometer base station

Instrument type: GEM Proton.

The GEM Proton is a portable high-sensitivity precession magnetometer.

The GEM Proton is a secondary standard for measurement of the Earth’s magnetic field with 0.01 nT resolutions, and 1 nT absolute accuracy over its full temperature range.

The base station data are sampled with 1 Hz frequency.

Appendix 2: Introduction to Spatially Constrained Inversion (SCI)

Model and inversion routine

The SkyTEM data have been processed and inverted using a spatially constrained inversion (SCI) in Aarhus Workbench, a unique software package initially developed at Aarhus University, Denmark. In the SCI algorithm, a group of time-domain EM (TEM) soundings are inverted simultaneously using 1-D models (Auken et al. 2002 & 2005, Viezzoli et al. 2008). Each sounding yields a separate layered model, but the models are constrained spatially on resistivity, see Figure 1 .

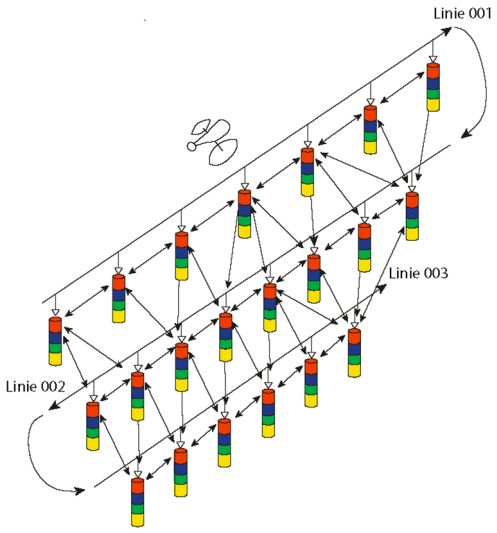

Figure 1. Schematic presentation of the SCI setup. Constraints connect not only soundings located along the flight line, but also those across them (figure from hgg.au.dk).

The result of the SCI inversion is a quasi-3D model that varies smoothly along and across the profiles. The SCI inversion is capable of simultaneously inverting the interleaved HM and LM measurements, yielding a conductivity model that combines the very good shallow depth resolution offered by the low moment data and the larger depth of investigation from the high moment data.

The SCI code is run in multi-layer, smooth-model mode, in which the layer thicknesses are fixed and the data are inverted only for resistivity. The SCI smooth-model inversion typically uses 20-30 layers. Smoothness constraints are applied on the variation of resistivity with depth, in additional to the lateral constraints between adjacent models. Multi-layer smooth-model inversion is slower to compute, but is usually able to provide a very close fit to the observed data.

In the model set-up the thickness of the first layer and the depth to the top of the deepest layer boundary is given. While computing the layer thicknesses, the first and last layer boundary scales the model thicknesses automatically using a log distribution.

The input data to the inversion are the LM & HM moments of the Z-component of EM data. Both moments are combined in a single inversion to increase the depth resolution. The initial model resistivity structure is a homogenous half-space model with an 500 ohmm starting resistivity.

Constraints are given as factors, i.e. a factor of 1.1 means that the parameter can vary between the starting value divided by/times 1.1 (Aarhus University).
The SCI inversion allows for horizontal and vertical constraints to be set for resistivities.
Horizontal constraints are scaled by distance using a reference distance and power function:

$$C = 1 + \left(C_{opt} - 1\right)\left(\frac{\Delta GPS}{Dist_{ref}}\right)^{n}$$

Where C is the used constraint, C_{opt} is the optimal constraint at a sounding distance of $Dist_{ref}$ and ΔGPS is the actual sounding distance.
The horizontal constraints are initially scaled by distance and a power function. Inversion for flight altitude is included after the first 5 inversion runs. The constraint on the processed flight height is set low and is only allowed a very limited variation.
The methodology for calculating the DOI is based on a recalculated Jacobian matrix from a 1D model (Christiansen and Auken, 2012). Working with global and absolute threshold values requires a relative, data-type, independent relation between the model space and data space, which we obtain by working in the logarithmic model and data spaces. For a given model, the DOI calculations solely include information from the part of the Jacobian relating to the observed data. This means that lateral or vertical model constraints or a priori information, which also contributes information to the model, is not included. The workflow includes the following steps:
1) Starting from a measured data set, the data is inverted into a smooth model. The inversion includes the data uncertainty, estimated from the data stack, and the regularization method of the chosen inversion algorithm.
2) The Jacobian for the sub-discretized model is calculated.
3) The Jacobian is finally used to compute the cumulated sensitivities from which we can deduct the DOI.

Data and noise model

The inaccuracy of TEM data is influenced by the ambient noise. This noise is reduced by selective stacking of delay time series and by applying appropriate filters in the receiver system.

Data insufficiency

For SkyTEM data, the insufficiency lies primarily in the limited delay time range that can be obtained. The earliest obtainable time gate is determined by the

turnoff of the Tx current, and the latest useful time gate is determined by the signal to noise ratio. Increasing the Tx moment will give better measurements at late times, and thus improve the depth penetration, but also increase the turnoff time and thus remove early-time gates, thereby making the near-surface resolution poorer. This trade-off is solved by transmitting an alternating sequence of (1) a low moment that can be turned off quickly to give good near-surface resolution, and (2) a high moment that will improve the signal-to-noise ratio at late times, thus improving depth penetration.

Model inconsistency

When using 1D models in the interpretation of SkyTEM data, inconsistency arises where the lateral gradient of conductivity is not small, e.g. typically in mining applications. However, also in environmental investigations, inconsistencies can arise, typically where near-surface good conductors have abrupt boundaries. Often such inconsistency is indicated by the data residual being high and one should look upon the inversion results with some caution at these locations. 3D effects can also reveal themselves by the so-called 'pant legs', i.e. conductive or resistive structures projecting at an angle of approximately 30 degrees from the horizontal at the edges of high contrast structures.